

Final Report on the Key Comparison CCM.P-K4.2012 in Absolute Pressure from 1 Pa to 10 kPa

Authors: Jacob Ricker (National Institute of Standards and Technology - NIST), Jay Hendricks (NIST), Thomas Bock (Physikalisch-Technische Bundesanstalt - PTB), Pražák Dominik (Czech Metrology Institute - CMI), Tokihiko Kobata (National Metrology Institute of Japan - NMIJ), Jorge Torres (Centro Nacional de Metrología - CENAM), Irina Sadkovskaya (DI Mendeleev Institute for Metrology - VNIIM)

ABSTRACT

The report summarizes the Consultative Committee for Mass (CCM) key comparison CCM.P-K4.2012 for absolute pressure spanning the range of 1 Pa to 10 000 Pa. The comparison was carried out at six National Metrology Institutes (NMIs), including National Institute of Standards and Technology (NIST), Physikalisch-Technische Bundesanstalt (PTB), Czech Metrology Institute (CMI), National Metrology Institute of Japan (NMIJ), Centro Nacional de Metrología (CENAM), and DI Mendeleev Institute for Metrology (VNIIM). The comparison was made via a calibrated transfer standard measured at each of the NMIs facilities using their laboratory standard during the period May 2012 to September 2013. The transfer package constructed for this comparison performed as designed and provided a stable artifact to compare laboratory standards. Overall the participants were found to be statistically equivalent to the key comparison reference value.

1. INTRODUCTION

This report summarizes the Consultative Committee for Mass (CCM) key comparison CCM.P-K4.2012 for absolute pressure spanning the range of 1 Pa to 10 000 Pa. The comparison was completed via calibration of a transfer standard carried out at six National Metrology Institutes (NMIs) during the period May 2012 to September 2013. Two nominally identical transfer standard packages were used in the comparison, Package B being circulated among participating laboratories and Package A remaining at the pilot lab in reserve as a back-up unit for the circulating package B.

Since the last key comparison in absolute pressure, CCM.P-K4.2000 [1], new national standards have been developed. These standards include manometers and non-rotating force-balanced piston gauges (FPG) that operate in the range of this comparison (1 Pa to 10 000 Pa absolute) [2]. It was decided that NIST's experience in the previous low pressure comparison and detailed knowledge in the design and construction of high-stability resonance silicon gauge transfer standard packages [3,4] made it well suited to be the pilot. NIST completed construction and testing of two new high stability transfer standard packages capable of absolute pressure measurements spanning the extended range of 1 Pa to 10 000 Pa.

The following sections provide brief descriptions of the laboratory standards, the design and construction of the transfer standard packages, the organization and chronology of the comparison, and the general calibration procedure required by the protocol. Methods for reduction and analysis of the calibration data were chosen to provide, as much as possible, uniform treatment of the results from individual laboratories, whether they were the pilot or another participant laboratory.

2. LABORATORY STANDARDS

The principal measurement methods tested by this comparison involved 5 types of laboratory standards: static expansion systems (SES), force-balanced piston gauges (FPG), piston gauges (PG), liquid-column manometers (manometers), and other calibrated transducers. SES, FPG, and PG are pressure generators while manometers and transducers are pressure measurement devices. Three participants (CENAM, NMIJ, and PTB) used static expansion systems as their laboratory standards and 2 participants used different types of laboratory standard manometers in which liquid-column heights were measured either by laser interferometry (VNIIM) or by ultrasonic interferometry (NIST). One participant, CMI, used the relatively new laboratory standard of an FPG. Three of the labs (PTB, CENAM, NMIJ) used a combination of standards. PTB used both SES and FRS5 (PG) standards, NMIJ used SES and a calibrated transducer, and CENAM used an SES and PG standards. Below each laboratories laboratory standard is described in the order in which the package was circulated.

2.1. NIST MERCURY AND OIL ULTRASONIC INTERFEROMETER MANOMETERS

The laboratory standards at NIST used in this key comparison are two Ultrasonic Interferometer Manometers (UIMs), a mercury UIM with a full-scale range of 160 kPa and an oil UIM [5, 6] with a full-scale range of 140 Pa. The unique feature of these manometers is that changes in height of the liquid columns are determined by an ultrasonic technique. A transducer at the bottom of each liquid column generates a pulse of ultrasound that propagates vertically up the column, is reflected from the liquid-gas interface, and returns to be detected by the transducer. The length of the column, which is proportional to the change in phase of the returned signal, is determined from the phase change and the velocity of the ultrasound [7, 8]. The manometers have large-diameter (75 mm – Hg UIM; 100 mm – oil UIM) liquid surfaces to minimize capillary effects, thermal shields to stabilize the temperature and minimize its gradients, and high-vacuum techniques to minimize leaks and pressure gradients. The mercury UIM employs a “W” or three-column design to correct for possible tilt. The oil UIM uses a four-column design equivalent to two parallel manometers that also function as orthogonal tilt meters.

The uncertainties for the NIST oil and mercury manometers [1,2,5] are given below:

Oil Ultrasonic Interferometer Manometer

$$(k = 1) \ u = \sqrt{(0.35 \times 10^{-3} \text{Pa})^2 + (5 \times 10^{-4} \times p)^2} \quad (1 \text{ Pa to } \leq 3 \text{ Pa})$$

$$(k = 1) \ u = \sqrt{(1.5 \times 10^{-3} \text{Pa})^2 + (18 \times 10^{-6} \times p)^2} \quad (> 3 \text{ Pa to } \leq 100 \text{ Pa})$$

Mercury Ultrasonic Interferometer Manometer

$$(k = 1) \ u = \sqrt{(3 \times 10^{-3} \text{Pa})^2 + (2.6 \times 10^{-6} \times p)^2} \quad (> 100 \text{ Pa to } 10 \text{ kPa}),$$

where p is the pressure in Pa.

2.2. PTB STATIC EXPANSION SYSTEM AND FRS5

At PTB, two laboratory standards were used: The static expansion system SE2 from 1 Pa to 30 Pa and the pressure balance FRS5 from 30 Pa to 11 kPa. The static expansion system, called SE2, in which pressures are generated by expanding gas of known pressure from a small volume into a much larger volume was described in detail in the publications [9,10,11]. The regular operational range of SE2 is 0.1 Pa up to 1 kPa.

These publications are outdated in terms of uncertainty evaluation as at that time the GUM was not yet existent. The uncertainty relevant for this comparison is:

$$(k = 1) \ u = 0.085 \% \text{ to } 0.071 \% \quad (1 \text{ Pa to } < 30 \text{ Pa}).$$

The evaluation of the FRS5 was described in publication [12]. The uncertainties can be approximated by the formula:

$$(k = 1) \ u = \sqrt{4.62 \times 10^{-4} \text{ Pa}^2 + p \times 1.08 \times 10^{-8} \text{ Pa} + p^2 \times 5.54 \times 10^{-10}} \quad (\geq 30 \text{ Pa to } 10 \text{ kPa}),$$

where p is the pressure in Pa.

It must be noted here that the laboratory for vacuum metrology is responsible only for the pressure scale up to 1 kPa in Germany. Above 1 kPa the official national primary standard is the mercury manometer of the pressure laboratory in Braunschweig, which was not used during this comparison. In the EURAMET.M.P-K4.2010 [13] (same range as this comparison) both laboratories of PTB took part with their respective standards being in full agreement, so that a sufficient link can be provided if necessary in the future.

2.3. CMI FORCE BALANCED PISTON GAUGE

The standard of CMI was a digital non-rotating piston gauge FPG8601 [14], manufactured by Fluke/DH-Instruments, USA and identified by serial number 107. The effective area was evaluated by the measurement of the piston-cylinder geometry and validated by the cross-floating techniques, see [15]. It is the same for both gauge, negative gauge and absolute modes. An intercomparison with the Slovak SMU was performed in 2002, with the Finnish MIKES in 2003, within EUROMET.M.P-S2, COOMET.M.P-K14, CCM.P-K4.2012 and also in the negative gauge pressure range within EURAMET.M.P-S12. The FPG was used in the range from 1 Pa to 10 kPa and operates with the following uncertainty:

$$(k = 1) \ u = 1.0 \times 10^{-2} \text{ Pa} + p \times 1.4 \times 10^{-5} \quad (1 \text{ Pa to } 10 \text{ kPa}),$$

where p is the pressure in Pa.

2.4. NMIJ STATIC EXPANSION SYSTEM AND CALIBRATED TRANSDUCER

NMIJ utilized a static expansion system for the range of 1 Pa to 100 Pa. A schematic of the NMIJ static expansion system is shown in the Figure 1a below. The system consists of four stainless steel chambers; A (Starting chamber, volume: about 0.2 L), B (Gas reservoir, 6 L), C (Sub expansion chamber, 10 L), and D (Main expansion chamber, 170 L). Chambers A and B are connected via a pneumatic all metal valve #2. Valves #3 and #5 are same as valve #2. A pressure gauge, which is calibrated against a pressure balance, is mounted on chamber B. Spinning rotor gauges (SRGs) and/or capacitance diaphragm gauges (CDGs) to be calibrated are mounted on chamber D. The pumping systems are connected to chambers B, C, and D, respectively. The ultimate pressures of each chamber are on the order of 10^{-7} Pa.

In the static expansion, the standard pressure is obtained by both an initial pressure stored in chamber A and volume ratios between chambers. A gauge is a heat source to a greater or lesser. Thus, there are no gauges on chamber A to avoid its thermal inhomogeneity. The initial pressure is evaluated by using the pressure indication of the pressure gauge on chamber B before the close of valve #2 and the pressure change induced by

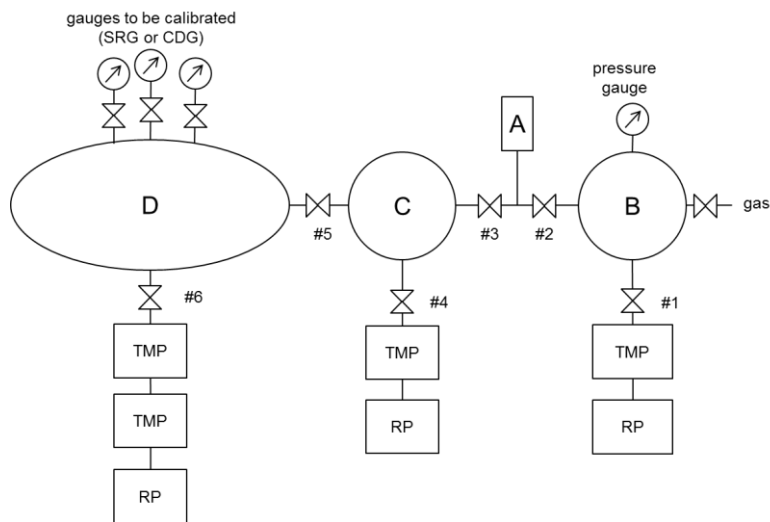


Diagram 1a. Schematic diagram of the NMIJ Static Expansion System.

the volume change inside the valve when the valve stem is moved to its closed position. Two volume ratios of chambers are used, one is chamber A to chamber C (sub expansion step) and the other is chamber A to chambers C and D (main expansion step). The volume ratio of the former case is about 50 and the latter about 900. A standard pressure ranging from 10^{-4} Pa to 150 Pa is obtained in chamber D after the sub expansion steps (0 to 2) followed by the main expansion step by varying the initial pressure from 10 kPa to 100 kPa. In this comparison, only the main expansion step was used to reduce the uncertainty of the standard pressure. The relative uncertainties of the static expansion system are:

$$\begin{aligned} (k = 1) \quad u &= 0.19 \% && (1 \text{ Pa to } < 10 \text{ Pa}) \\ (k = 1) \quad u &= 0.09 \% && (\geq 10 \text{ Pa to } 150 \text{ Pa}). \end{aligned}$$

For the range of 300 Pa to 10 kPa, NMIJ used two differential pressure gauges calibrated by a double pressure balance as standards. A 1 kPa resonant silicon gauge (RSG) was used for 300 Pa to 1 kPa and a 10 kPa RSG was used for 1 kPa to 10 kPa.

Each of the gauges was calibrated under the line pressure of 100 kPa (absolute mode) in the double-pressure-balance system. Then the low pressure port was evacuated and used as an absolute pressure gauge (with a line pressure of 0 kPa). The indication of the gauge shows some dependence on the line pressure, so the dependency was evaluated and applied as a correction.

The uncertainty for this measurement system using differential pressure gauges is as follows:

$$\begin{aligned} (k = 1) \quad u &= 0.060 \text{ Pa} + p \times 10 \times 10^{-6} && (300 \text{ Pa to } \leq 1 \text{ kPa}) \\ (k = 1) \quad u &= 0.075 \text{ Pa} + p \times 27.5 \times 10^{-6} && (> 1 \text{ kPa to } 10 \text{ kPa}), \end{aligned}$$

where p is the pressure in Pa.

2.5. CENAM STATIC EXPANSION SYSTEM AND PISTON GAUGE

CENAM utilized a static expansion system, referred to as SEE-1, for this comparison. SEE-1 has 4 volumes, as described in the table below and shown in the figure 1b. These volumes are used to obtain different expansion paths [16].

Identification	Nominal volume
V ₁	0.5 L
V ₂	50 L
V ₃	1 L
V ₄	100 L

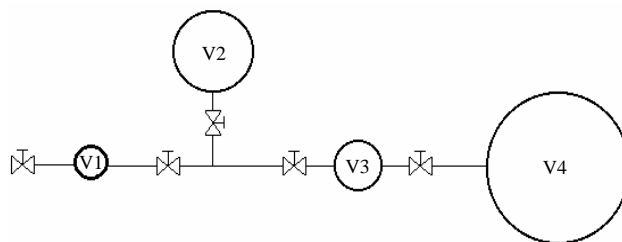


Diagram 1b. Schematic diagram of the CENAM Static Expansion System.

The SEE-1 calibration chamber is shown in the figure as V4. It is possible to perform various expansions before the calibration pressure is achieved. The table below shows the different expansion paths in the SEE-1. Additionally, a volume V_x is included to correct for the volume of tubing between volumes V1, V2, and V3.

Identification	Expansion path
f_A	$V_1 \rightarrow V_1 + V_x + V_2$
f_B	$V_1 \rightarrow V_1 + V_x + V_2 + V_3$
f_C	$V_3 \rightarrow V_3 + V_4$

Uncertainties ($k = 1$) for SEE-1 in this comparison are described as:

$$\begin{aligned} (k = 1) \quad u &= 0.175 \% && (1 \text{ Pa to } 30 \text{ Pa}) \\ (k = 1) \quad u &= 0.105 \% && (70 \text{ Pa to } 1 \text{ kPa}) \end{aligned}$$

Additionally CENAM, used a pressure balance for the range from 3 kPa to 10 kPa. The pressure balance was manufactured by DHI, model number 7607, with serial number 122 with Piston cylinder: 231 and Masses: 2018. The device operates with the following uncertainty:

$$\begin{aligned} (k = 1) \quad u &= 1.5 \times 10^{-2} \text{ Pa} + p \times 7.5 \times 10^{-6} && (3 \text{ kPa to } 7 \text{ kPa}) \\ (k = 1) \quad u &= p \times 7.5 \times 10^{-6} && (10 \text{ kPa}), \end{aligned}$$

where p is the pressure in Pa.

2.6. VNIIM MERCURY AND OIL LASER INTERFEROMETER MANOMETERS

The laboratory standards at VNIIM used in this key comparison are two liquid manometers: a Laser Interferometric Oil Manometer (LIOM) with a full-scale range of 1000 Pa and a Laser Interferometric Mercury Manometer (LIMM) with a full-scale range of 130 kPa. The operation principal of LIOM was presented in [17]. LIOM has a stainless steel body with two 40 mm diameter cylindrical holes. The laser beams in the Michelson's interferometer scheme reflect from free oil surfaces. The unique feature of LIOM is the application of special floats damping the surface waves to provide reliable performance of the fringe counting system. The floats for mercury manometer are made of cat's eye type and have protective rings stabilizing the contrast of fringes [18].

The uncertainties for the VNIIM oil and mercury manometers are given as:

Laser Interferometric Oil Manometer

$$(k = 1) \quad u = 3.6 \times 10^{-3} \text{ Pa} + p \times 0.5 \times 10^{-4} \quad (1 \text{ Pa to } 1 \text{ kPa})$$

Laser Interferometric Mercury Manometer

$$(k = 1) \quad u = 4.0 \times 10^{-1} \text{ Pa} + p \times 4.9 \times 10^{-6} \quad (3 \text{ kPa to } 10 \text{ kPa}),$$

where p is pressure in Pa.

3. TRANSFER STANDARDS

On the basis of earlier comprehensive reviews of pressure transducer performance [3,19], two types of gauges were selected as the transfer standards, namely, resonant silicon gauges (RSGs) for their good long-term stability and capacitance diaphragm gauges (CDGs) for their high-precision. The RSGs are a type of MEMS (micro-electromechanical systems) sensor that have excellent calibration stability, are resistant to mechanical shock, and are only moderately susceptible to overpressure although they are rather sensitive to tilt ($\approx 0.4 \text{ Pa/mrad}$). However they lack sufficient pressure resolution to cover the entire range of the comparison. The CDGs have superior pressure resolution and, because of their all-metal construction, are rugged and resistant to overpressure but lack the desired calibration stability required by the comparison. The transfer standard package uses both types of gauges, two CDGs to provide redundancy and high resolution at low pressures, and two RSGs to provide redundancy and excellent calibration stability. Good calibration stability was accomplished over the entire pressure range by re-scaling the CDG response to that of the RSGs at an overlapping pressure.

The two RSGs selected for the comparison had full-scale ranges of 10 000 Pa and were combined with two CDGs each with a full-scale range of 133 Pa. Both RSGs and CDGs are of differential type with an ion pump to provide the vacuum reference pressure required for a comparison in absolute pressure.

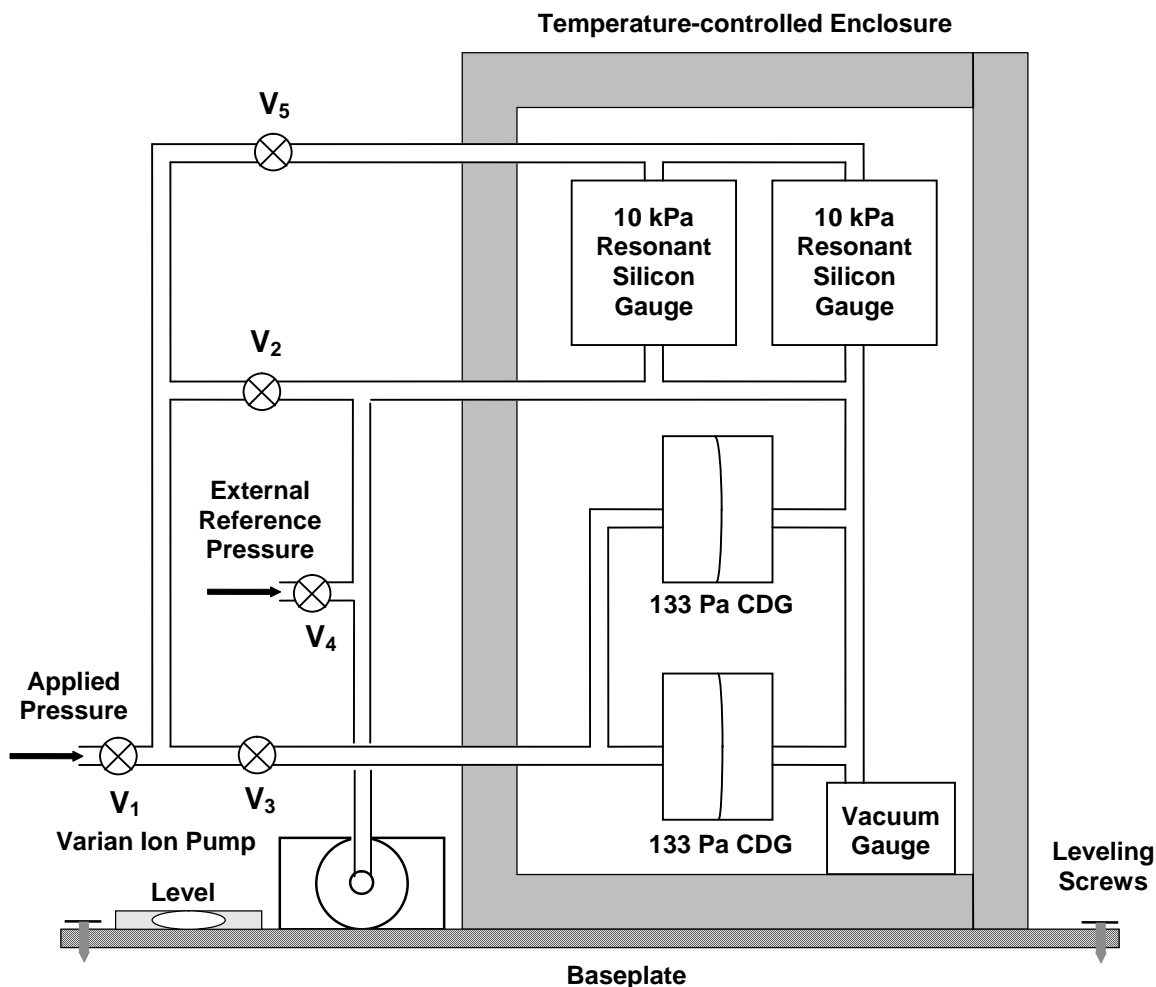


Figure 2a. Schematic diagram of the pressure transducer package (PTP).

The transfer standard package consisted of two parts, a pressure transducer package (PTP) and a support electronics package (SEP), which included an internally mounted computer (see Figure 2a and Figure 2b). The PTP included four differential transducers housed in a temperature-controlled enclosure, a calibrated 100 Ω platinum resistance thermometer (PRT) to measure the interior temperature of the enclosure, and an ion pump and reference-pressure vacuum gauge for absolute mode calibrations. All-metal plumbing was used throughout the PTP including metal bellows-sealed valves and metal bellows connections to each transducer to minimize mechanical strain. The valves included external isolation valves V₁ and V₄, internal isolation valves for the CDGs (V₃) and RSGs (V₅), and an internal bypass valve V₂ between the pressure and reference side of the gauges. The gauges and internal plumbing were maintained under vacuum during shipment or storage, but with all internal valves open to avoid overpressurization of the gauges in the event of a leak to atmosphere. The tilt orientation of the PTP during calibration of the RSGs was monitored by means of sensitive bubble levels mounted on the PTP base plate and any observed changes were corrected using the leveling screws.

The SEP included a temperature controller for the transducer enclosure, signal conditioning electronics for the CDGs, a controller for the ion pump, and a digital voltmeter (DVM) for measuring analog signals from the CDGs, the calibrated PRT, and the reference vacuum gauge. The enclosure temperature was controlled (typical stability is better than 0.05 °C) by means of a heat pump and a Wheatstone bridge mounted inside the enclosure where the bridge included an uncalibrated PRT and an adjustable resistor in two of its arms (not shown in Figure 2a).

A rack-mount computer was used for controlling the acquisition of data from the RSGs and the DVM during calibration. The time required to obtain one set of readings was approximately 55 seconds. Because of their accuracy ($\approx 0.01\%$), the readings of the RSGs were multiplied by a scale factor before display and storage on the computer in order to increase the level of confidentiality for the pilot laboratory data. The RSG data submitted by the participants were multiplied by $1/(\text{scale factor})$ during subsequent data reduction in order to restore the original readings.

For interlaboratory shipment, the PTP and SEP were mounted in specially designed commercial containers that conform to ATA (Air Transport Association) and pertinent military standard specifications for vibration and shock isolation.

4. ORGANIZATION OF THE KEY COMPARISON

The present key comparison in absolute pressure (CCM.P-K4.2012) was organized with two nominally identical transfer standard packages. Transfer standard package B was circulated to participants while transfer standard package A remained at NIST to serve as a back-up should something unfortunate happen to the circulating package.

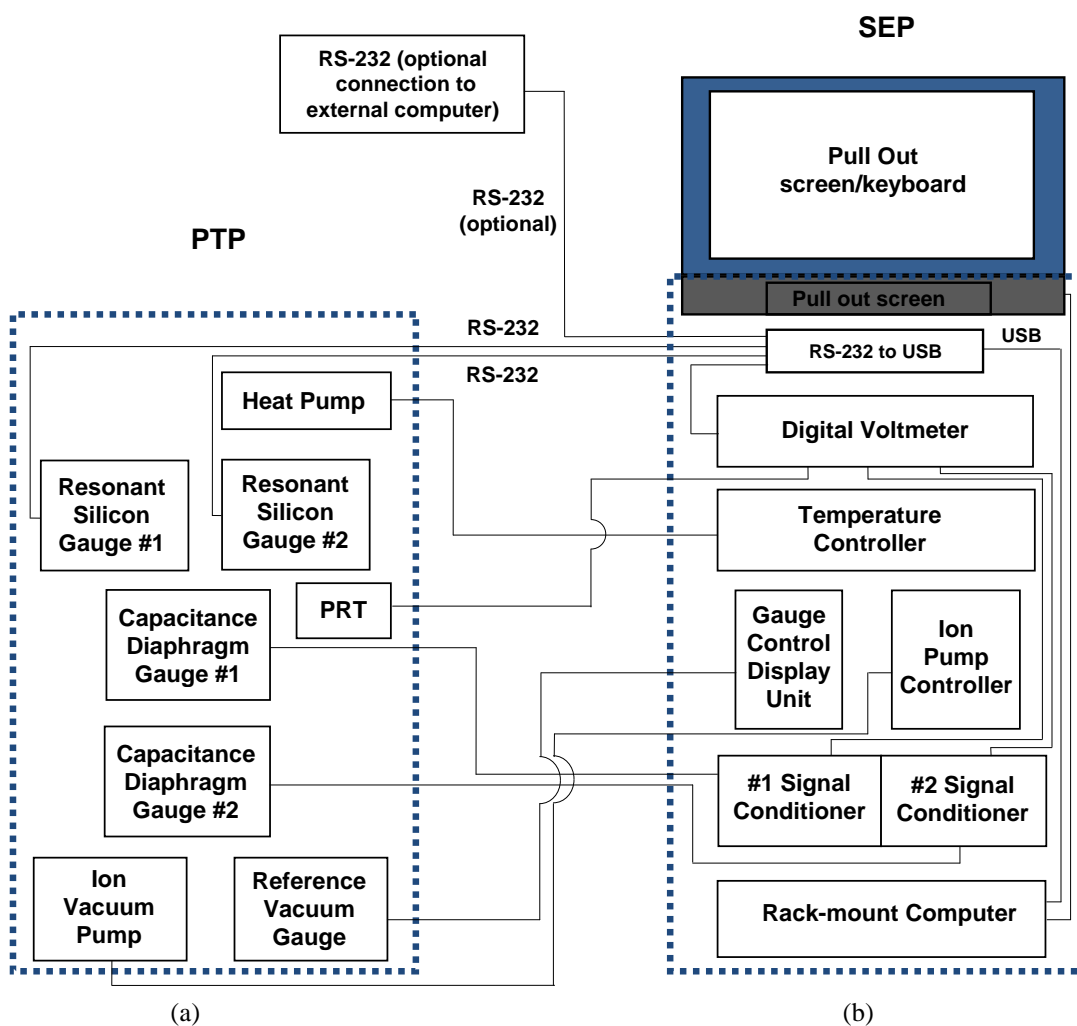


Figure 2b. Schematic diagram of the electrical connections between the PTP (a), and the support electronics package (SEP) (b).

4.1. CHRONOLOGY OF THE MEASUREMENTS

Table 1 presents the actual chronology of calibrations during the measurement phase of the comparisons. The start and end dates refer to the time period during which each NMI had possession of the transfer standard. In all cases, the NMI measurement data (5 runs) was collected within a 2 week time interval. The total time required to complete the measurement phase of the absolute pressure comparison was eighteen months, which is approximately two months longer than initially projected.

Table 1. Chronology of measurements during the key comparison in absolute pressure.

Laboratory	Transfer Std. Package	Calibration Start Date	Calibration End Date
Pilot - NIST	A,B	7 January 2012	30 April 2012
NMI 1 - PTB	B	11 May 2012	19 June 2012
NMI 2 - CMI	B	21 June 2012	4 September 2012
NMI 3 - NMJ	B	19 September 2012	26 November 2012
Pilot - NIST	A,B	7 December 2012	24 January 2013
NMI 4 - CENAM	B	20 Feb 2013	27 March 2013
NMI 5 - VNIIM	B	5 April 2013	28 April 2013
NMI 6 - NMISA	B	7 May 2013	3 June 2013
Pilot - NIST	A, B	13 June 2013	12 September 2013

4.2. PROBLEMS DURING THE COMPARISONS

Overall, the transfer standards package A and B performed well. However, the ion pump power supply on the transfer standard package B stopped working while at CENAM. Measurements were completed with a turomolecular pump provided by CENAM. The function of the pump is to maintain the reference vacuum on the differential CDG and RSG gauges. The vacuum is measured with the vacuum gauge shown in Figure 1 and the values for the reference vacuum with the turbo molecular pump were very similar to the values obtained by NIST and other NMIs that were taken with the properly function ion pump. NMISA encountered problems with data collection and data retrieval unrelated to the transfer standard package and withdrew from the comparison and no data was submitted.

5. GENERAL CALIBRATION PROCEDURE

The protocol for the key comparison required that each laboratory calibrate the transfer standard with nitrogen gas at the following nominal absolute pressures in ascending order: 1 Pa, 3 Pa, 10 Pa, 30 Pa, 100 Pa, 300 Pa, 1000 Pa, 3000 Pa, 7000 Pa, 10 000 Pa. The nominal reference or base pressure provided by the ion vacuum pump was to be $\approx 10^{-3}$ Pa. The actual absolute pressures realized at the transfer standard gauges by the participant's pressure standard was to be within 2 % of the target pressures. Optional calibration data could also be taken at 7 Pa, 70 Pa, and 700 Pa.

A total of **five calibration runs** were required, proceeding from lowest to highest pressures and each run taken on a different day. Within a calibration run, **five repeat data points** of pressure and temperature readings of the transfer standard and laboratory standard were required at each target pressure. At the beginning of each calibration run, **ten data points** of zero-pressure readings for the transfer standard gauges were required to be taken with the PTP isolated from the participant's calibration system (valves V_1 and V_4 closed) and with internal isolation valves V_3 and V_5 and bypass valve V_2 open. These data were needed to correct calibration data obtained with liquid-column manometers for zero-pressure offsets. An additional ten repeat sets of zero-pressure readings were to be taken at the end of each run in order to monitor zero drift in the four transducers during calibration. The calibration procedure also included the option of recording **five points** of zero-offset readings for the gauges just prior to establishing each target pressure. These readings, which were taken with the external and internal

isolation valves of PTP open and bypass valve V_2 closed, were needed to correct zero offsets in calibration data obtained with static expansion systems.

The format for reporting calibration data followed the measurement sequence dictated by the data acquisition software. The sequence for each set of associated readings of the transfer standard and the participant's laboratory standard was:

$$Point\ No.\quad p_{CDG1}\quad p_{CDG2}\quad p_{RSG1}\quad p_{RSG2}\quad p_{REF}\quad T_{PTP}\quad P_{NMI}\quad T_{NMI}\quad u_{NMI}(k=1)$$

where the meaning of subscripts for pressures p (gauges), p_{REF} (reference pressure), P (laboratory standard at each NMI), and temperatures T (Pressure Transducer Package or PTP), T (laboratory standard at each NMI) and uncertainty u of the NMI laboratory standard are self-explanatory. All calibration data were transmitted to the pilot laboratory in the form of spreadsheet files.

6. REDUCTION AND ANALYSIS OF THE REPORTED DATA

The reduction and analysis of the key comparison data required that the following factors be addressed:

- Zero-pressure offsets (Section 6.1)
- Thermal transpiration effects (Section 6.2)
- Deviations from target pressures (Section 6.3)
- Calibration shifts in the capacitance diaphragm gauges (Section 6.4)
- Calculation of the predicted gauge readings (Section 6.5)

Additionally, the methods for estimating uncertainties (Sections 6.6 and 6.7) and evaluating degrees of equivalence (Section 6.8) are also described. All of these factors were determined by the pilot lab while the participants were responsible for all correction factors individual to their standard (i.e. head correction, Hg vapor pressure, etc).

6.1. CORRECTIONS FOR ZERO-PRESSURE OFFSETS

The first step in reducing the comparison data was to correct the readings of each gauge, i , for their zero-pressure offset. The index i is equal to either 1 or 2 and refers to either, CDG1 and CDG2, or RSG1 and RSG2 (see Figure 1). At a given target pressure during calibration run r , the corrected reading of gauge i for data point l is given by:

$$p'_{irl} = p_{irl} - \langle p_{ir} \rangle_{10} + p_{REF_{rl}} \quad (1),$$

where p_{irl} is the uncorrected gauge reading, $\langle p_{ir} \rangle_{10}$ is the mean of 10 zero-pressure readings taken prior to the start of calibration run r , and $p_{REF_{rl}}$ is the transfer standard's reference pressure reading during data point l .

6.2. CORRECTIONS FOR THERMAL TRANSPARATION EFFECTS

The difference in temperature of a laboratory standard and the transfer standard gauges can give rise to significant thermal transpiration effects at low pressures [20]. In the present comparison the magnitude of this effect will vary since the laboratory standards were operated at somewhat different temperatures (see Figure 3). The effect of different operating temperatures was minimized by determining the pressure that a laboratory standard would measure/generate if it were operating at the same temperature as the transfer standard gauges.

At a given target pressure during calibration run r , the corrected reading of a NMI's laboratory standard for data point l is given to a good approximation by the Takaishi-Sensui equation [21]:

$$P'_{NMI(j)rl} = P_{NMI(j)rl} f_{tt} = P_{NMI(j)rl} \frac{(aY^2 + bY + cY^{0.5} + 1)}{\left(aY^2 + bY + cY^{0.5} + \left(\frac{T_{NMI(j)rl}}{T_{PTP_{rl}}} \right)^{0.5} \right)} \quad (2a),$$

Where for each NMI j , $P_{NMI(j)rl}$ represents the uncorrected pressure measured/generated by the laboratory standard operating at absolute temperature $T_{NMI(j)rl}$, $T_{PTP_{rl}}$ is the absolute temperature (K) of the transfer standard gauge, a , b , and c , are temperature-independent gas-species dependent constants, and the parameter Y is defined as

$$Y = \frac{P_{NMI(j)rl} \times d}{133.322 \left(\frac{T_{NMI(j)rl} + T_{PTP_{rl}}}{2} \right)} \quad (2b)$$

and d is the internal diameter of the gauge inlet tubing in mm. The interior temperature of the transfer standard enclosure as measured by the PRT is assumed to closely approximate the temperature of each gauge. It can be seen in Figure 2 that the temperature of the transfer standards was significantly more uniform than the operating temperature of the laboratory standards at different NMIs.

The corrections to the measured/generated pressures (factors f_{tt}) are based on $d = 4.6$ mm and the following reported values for nitrogen: $a = 1.2 \times 10^6$, $b = 1.0 \times 10^3$, and $c = 14$ [20,21]. The corrections are largest at lowest pressures and are small, but significant for this comparison. For example at 1 Pa the value of f_{tt} , from equation (2a), ranged from 0.9990 to 1.0041. Because of the small size of the correction, and an estimated uncertainty of this equation $U_{tt} < 5$ %, the component of uncertainty on pressure is negligible.

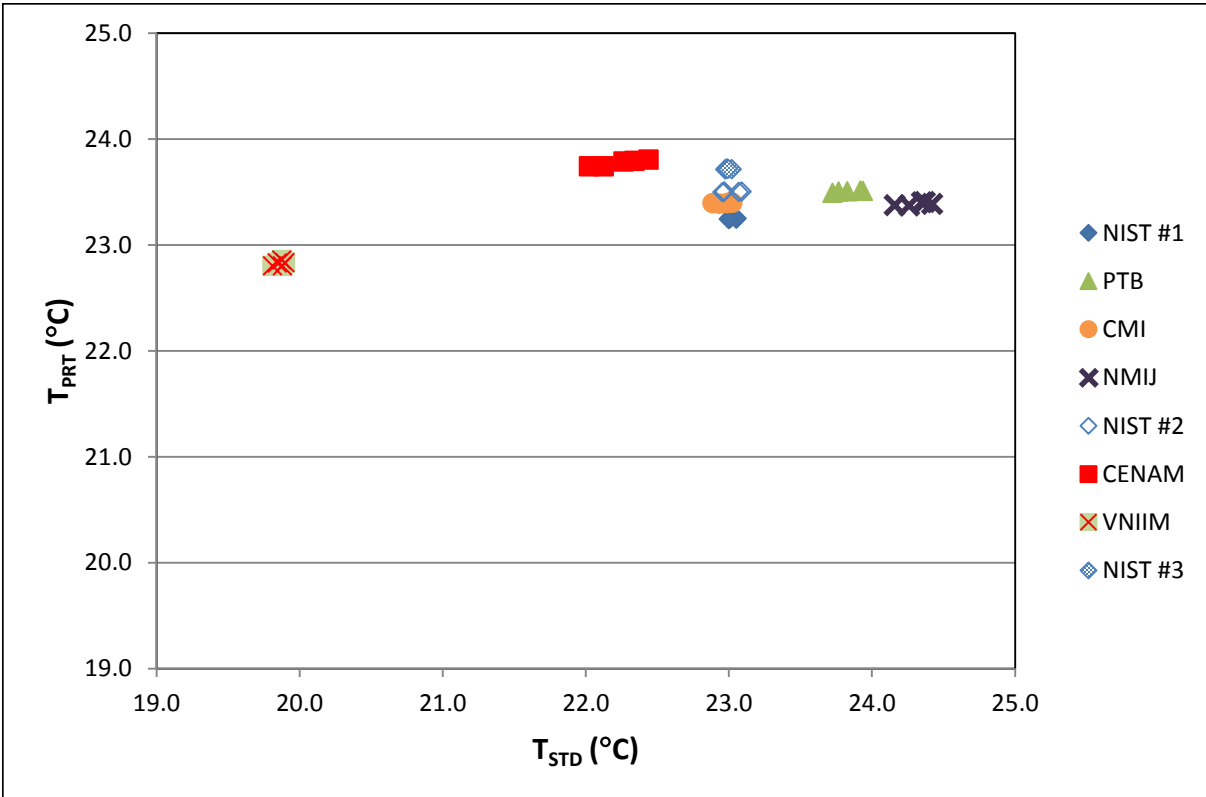


Figure 3. Temperature of laboratory standards vs temperature of transfer standard.

As seen in Figure 3, the performance of the transfer package temperature is significantly more stable than the laboratory standard's temperatures at all the participating labs. However some variability was seen in the setpoint of the temperature controller as evident from the shift in T_{PRT} across the three pilot lab measurements. Since the shift is unidirectional, and no directional shifts were exhibited in the pressure data, the uncertainty due to this variation is assumed to be covered by the long term stability of the package.

6.3. CALCULATION OF CALIBRATION RATIOS

The transfer standard gauges are nominally linear devices and so the ratio of transfer standard reading to laboratory standard reading will be essentially independent of pressure for a range of pressures about each target value. These ratios form the basis for the comparison of laboratory standards from different NMIs.

At each target pressure during calibration run r the mean ratio of 5 repeat readings of transfer standard gauge i and NMI laboratory standard j is given by

$$b_{ijr} = \frac{1}{5} \sum_{l=1}^5 \frac{p'_{irl}}{P'_{NMI(j)rl}} \quad (3),$$

where p'_{irl} and P'_{jrl} are the “simultaneous” readings of the gauge and laboratory standard, respectively. The mean of b_{ijr} for 5 calibration runs defines a *calibration ratio* given by

$$b_{ij} = \frac{1}{5} \sum_{r=1}^5 b_{ijr} = \frac{1}{25} \sum_{r=1}^5 \sum_{l=1}^5 \frac{p'_{irl}}{P'_{NMI(j)rl}} \quad (4).$$

The overall calibration ratio b_{ij} may be used to calculate a normalized average gauge reading p_{ij} by setting the pressure measured/generated¹ by each laboratory standard $P_{NMI(j)}$ equal to the target pressure, p_t .

$$p_{ij} = b_{ij} P_{NMI(j)} = b_{ij} p_t \quad (5)$$

6.4. RE-SCALING THE CDG READINGS

Figures 4 and 5 present the calibration ratios for RSGs and CDGs in the transfer standard package as determined by three repeat calibrations at NIST. The RSGs offer superior stability, even at 100 Pa, where the shifts in their response between calibrations were about a factor of 50 smaller than similar shifts exhibited by the CDGs. The calibration shifts of the CDGs can be reduced significantly by re-scaling their readings so they equal those of the RSGs at an overlapping pressure. For this comparison, the readings of each CDG at 100 Pa were re-scaled to a single RSG. For stability, CDG1 was always paired with RSG1 and CDG2 with RSG2.

At target pressures $p_t \leq 100$ Pa, the re-scaled reading of capacitance diaphragm gauge i may be expressed for each NMI, j , as

$$p'_{CDG_{ij}}(p_t) = p_{CDG_{ij}}(p_t) * \frac{p_{RSG_{ij}}(100)}{p_{CDG_{ij}}(100)} \quad (6a),$$

¹ The measured or generated pressure is the calculated value obtained from each NMI's laboratory standard, corrected for any effects that may be individual to that type of standard (i.e. mercury vapor pressure).

where $p_{CDG_{ij}}(p_t)$ is the normalized CDG reading before re-scaling. This equation may be re-expressed in terms of calibration ratios by means of Equation (5) as

$$b'_{CDG_{ij}}(p_t) = b_{CDG_{ij}}(p_t) * \frac{b_{RSG_{ij}}(100)}{b_{CDG_{ij}}(100)} \quad (6b),$$

where $b_{CDG_{ij}}(p_t)$ and $b'_{CDG_{ij}}(p_t)$ are the respective calibration ratios for capacitance gauge i before and after re-scaling, and $b_{RSG_{ij}}(100)$ and $b_{CDG_{ij}}(100)$ are the calibration ratio for RSG i and CDG i at a pressure of 100 Pa.

The rescaled values for the CDGs are shown in Figure 6. A comparison between Figures 5 and 6 show a significant improvement in the stability of the CDGs between successive runs. For this comparison, a rescaled value of $b'_{CDG_{ij}}$ is used for all pressures below 100 Pa and $b_{RSG_{ij}}$ is used for all pressures 100 Pa to 10 kPa, or

$$b'_{ij}(p_t) = \begin{cases} b_{RSG_{ij}}(p_t) & \text{for } p_t \geq 100 \text{ Pa} \\ b'_{CDG_{ij}}(p_t) & \text{for } p_t < 100 \text{ Pa} \end{cases} \quad (7).$$

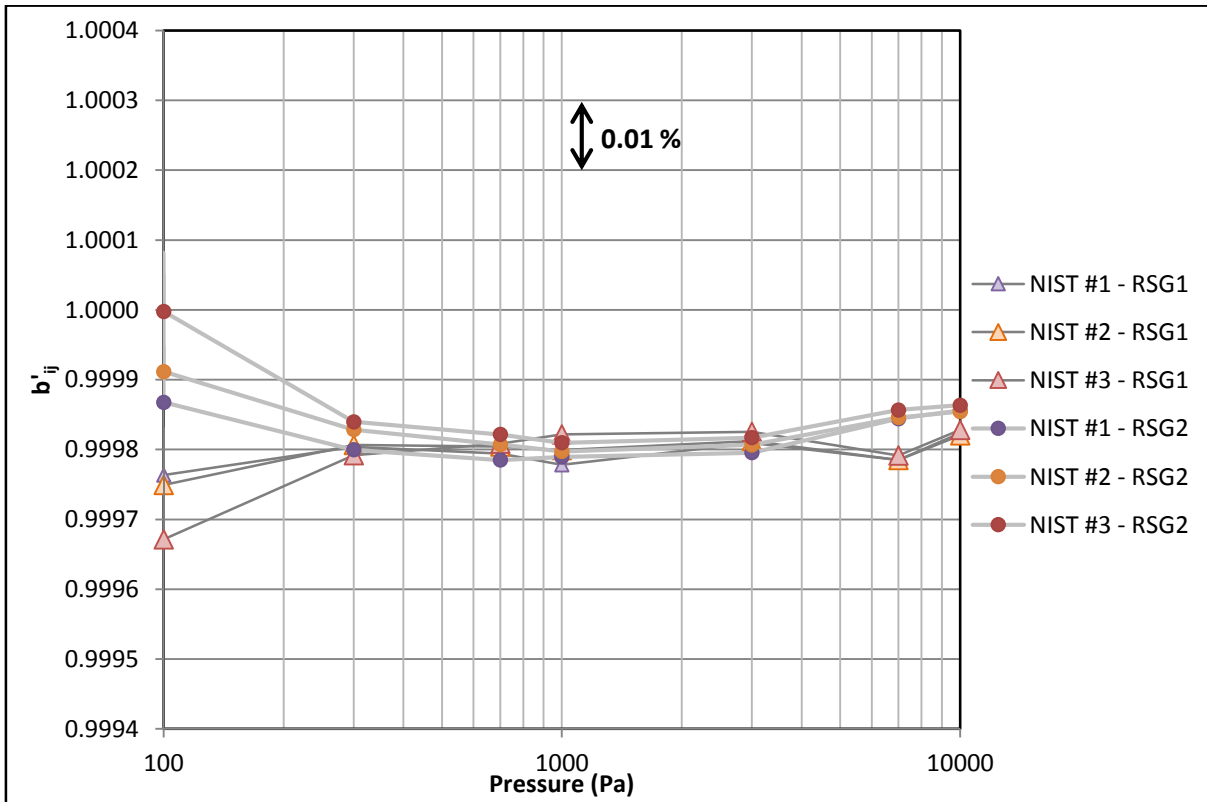


Figure 4. Calibration ratios, $b'_{ij}(p_t)$, for RSGs in Transfer Package B as a function of pressure.

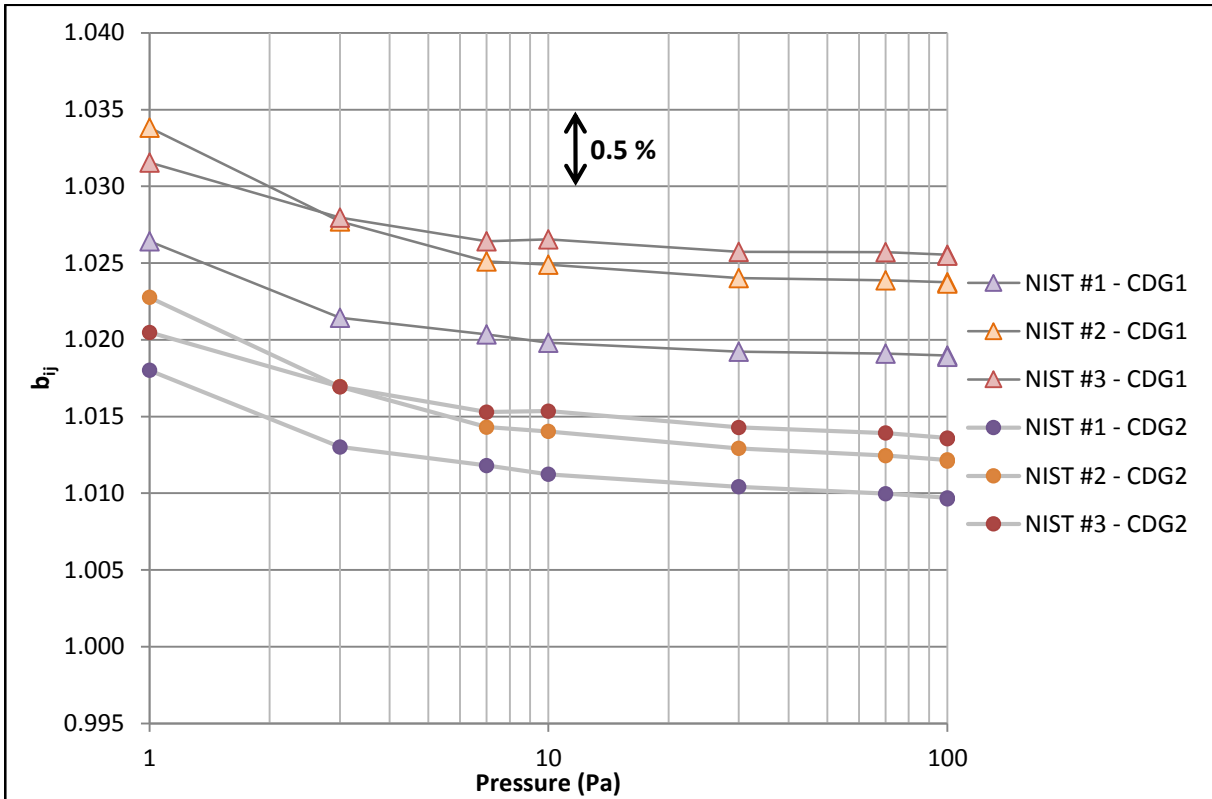


Figure 5. Calibration ratios, $b_{CDG_{ij}}(p_t)$, for CDGs in Transfer Package B as a function of pressure before rescaling to RSGs.

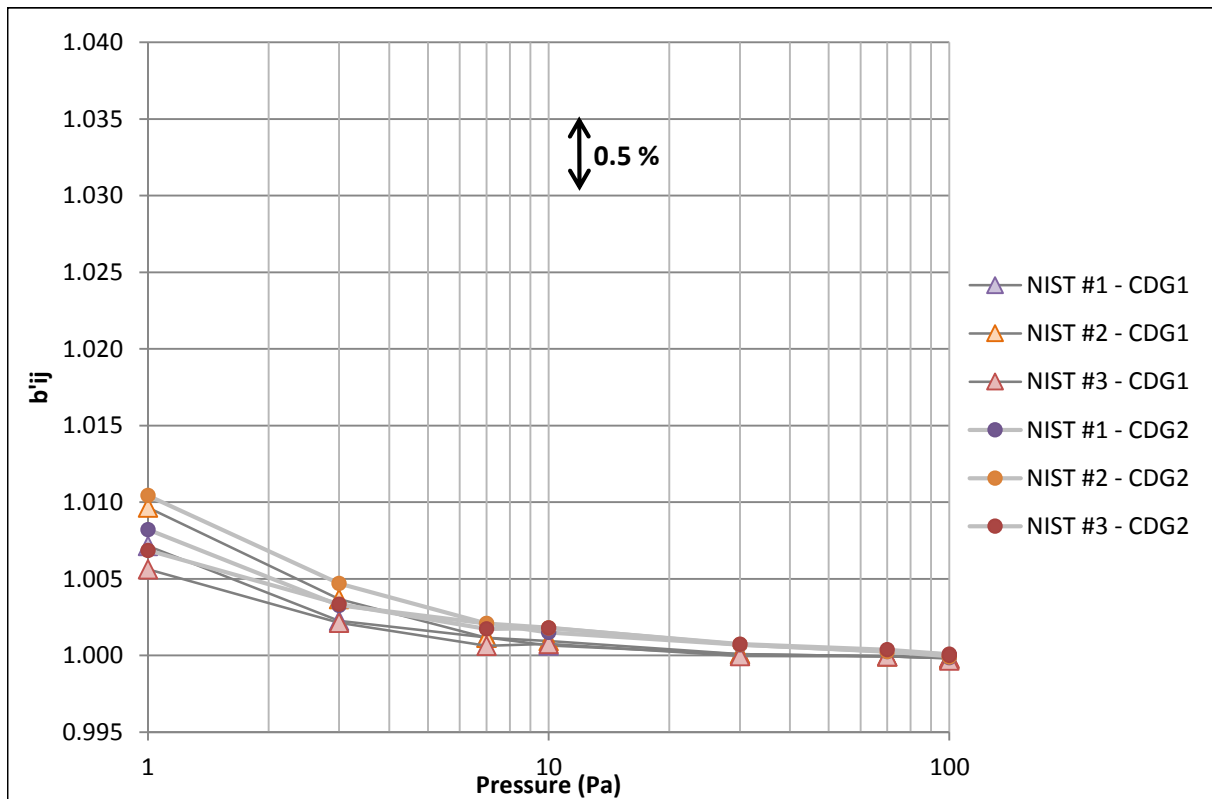


Figure 6. Calibration ratios, $b'_{CDG_{ij}}(p_t)$, for CDGs in Transfer Package B as a function of pressure after rescaling to RSGs.

6.5. CALCULATION OF THE PREDICTED GAUGE READINGS

Degrees of equivalence [22] of the laboratory standards for absolute pressure can be expressed quantitatively by comparing pressure readings of the transfer standard gauges. The basic method adopted here is to use the calibration ratios to predict gauge readings that would be observed had the target pressure generated been equal for each NMI's laboratory standard. The difference between the calculated predicted gauge readings for the different laboratory standards is taken as a surrogate for the difference between laboratory standards².

At all target pressures there are two gauges ($i = 1, 2$) and there will be two gauge readings for each pressure measured/generated by laboratory standard j and, according to Equation (5), these may be expressed as:

$$p_{ij} = b'_{ij} P_{\text{NMI}(j)} \quad (8),$$

where b'_{ij} is the rescaled calibration ratio for gauges i , p_{ij} are their respective pressure readings, and $P_{\text{NMI}(j)}$ is the measured/generated pressure using the laboratory standard.

The predicted gauge readings, p'_{ij} , for each laboratory can be calculated by setting the pressure measured/generated by each laboratory standard P_j equal to the target pressure, p_t , i.e., when $P_{\text{NMI}(j)} = p_t$. The predicted gauge readings are defined as:

$$p'_{ij} = b'_{ij} p_t \quad (9).$$

The results for p'_{ij} from individual laboratories are presented in Section 7.1.

At each target pressure, there are two values for the normalized gauge reading (e.g., for CDG1 and CDG2, etc.) and so a mean gauge reading p_j was calculated as a simple arithmetic mean:

$$p_j = \frac{p'_{1j} + p'_{2j}}{2} \quad (10).$$

For the pilot laboratory, a single value of p_j is calculated as an arithmetic mean of six values of p_{jn} . The values of p_{ijn} are determined via Equation (9) using calibration ratios b_{ijn} obtained from three calibrations ($n = 1, 2, 3$) of two gauges ($i = 1, 2$), therefore equation (10) becomes:

$$p_j = \frac{p'_{1j1} + p'_{2j1} + p'_{1j2} + p'_{2j2} + p'_{1j3} + p'_{2j3}}{6} \quad (11)$$

for the pilot lab only, $j = \text{pilot (NIST)}$.

6.6. ESTIMATES OF UNCERTAINTIES IN THE NORMALIZED GAUGE READINGS

The combined uncertainty³ in the normalized gauge readings calculated using Equation (9) may be estimated from the root-sum-square of three component uncertainties [23, 24],

² This method assumes linearity of the transfer standard gauge about the target pressure. For this comparison, participants were instructed to achieve a pressure within $\pm 2\%$ of the target pressure. This approximation results in negligible uncertainty in this comparison, change in slope over two lowest pressures (largest nonlinearity) results in 7×10^{-5} Pa uncertainty at 1 Pa.

³ Uncertainty refers to standard uncertainty unless noted otherwise.

$$u_c(p_{ij}) = \sqrt{u_{std}(p_{ij})^2 + u_{rdm}(p_{ij})^2 + u_{lts}(p_{ij})^2} \quad (12),$$

where $u_{std}(p_{ij})$ is the Type B uncertainty in p_{ij} due to systematic effects in laboratory standard j , $u_{rdm}(p_{ij})$ is the Type A uncertainty in p_{ij} due to the combined effect of short-term random errors of transfer standard gauge i and laboratory standard j during calibration, and $u_{lts}(p_{ij})$ is the uncertainty arising from long-term shifts in the response function of gauge i during the course of the comparison. Figure 7 presents the estimated relative uncertainties in pressure in the laboratory standards, as stated by the participants for target pressures used in the comparison.

The relative uncertainty in p_{ij} due to short-term random effects during calibration can be estimated from the corresponding uncertainties in the calibration ratios via Equation (9):

$$\frac{u_{rdm}(p_{ij})}{p_{ij}} = u_{rdm}(b'_{ij}) \quad (13).$$

Similarly the relative uncertainty in p_{ij} due to long-term shifts in gauge response between calibrations is given by

$$\frac{u_{lts}(p_{ij})}{p_{ij}} = u_{lts}(b'_{ij}) \quad (14),$$

where b'_{ij} is the normalized calibration ratio for gauge i .

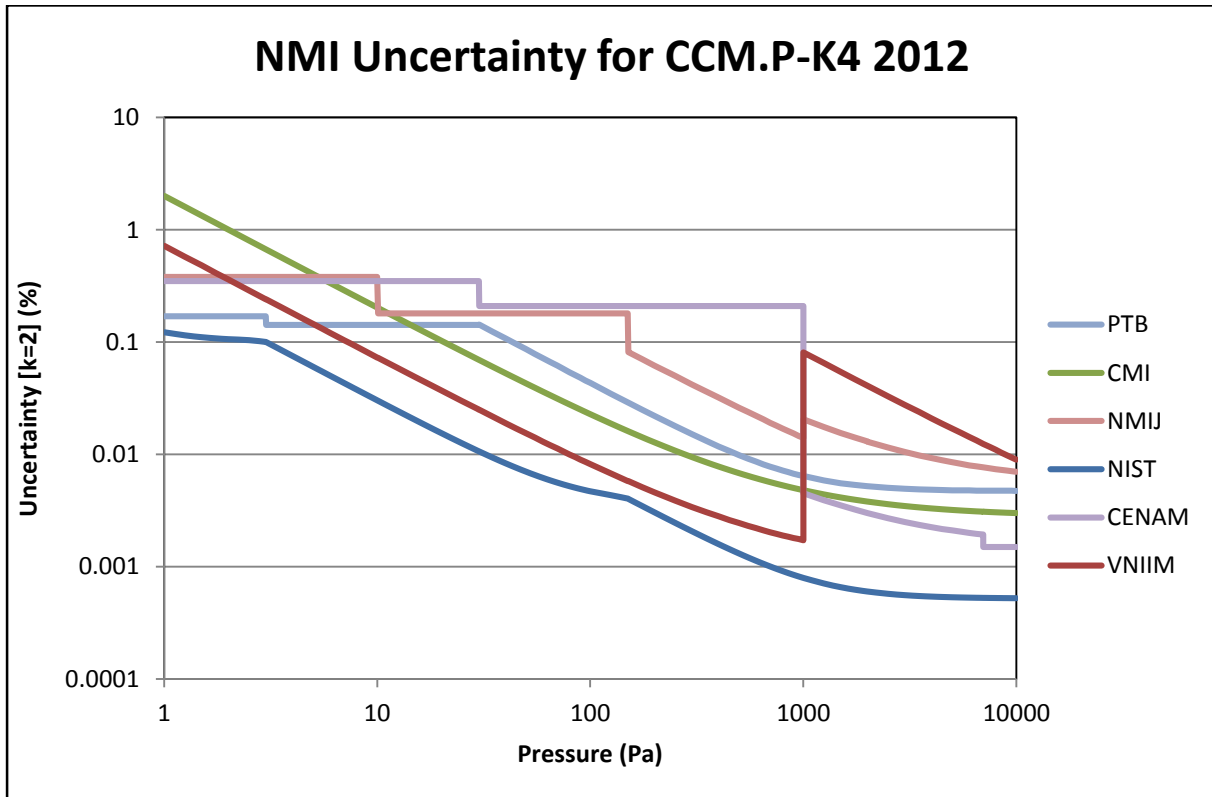


Figure 7. NMI relative uncertainty due to systematic effects in laboratory standards at the participating laboratories as a function of pressure.

For pressures above 100 Pa, the short-term random uncertainty in a calibration ratio, b_{ij} , as given by Equation (4), was estimated by a Type A evaluation as

$$u_{rdm}(b'_{ij}) = \frac{\sigma_{ijr}}{\sqrt{5}} \quad (15)$$

for $p_t > 100$ Pa, where σ_{ijr} is the standard deviation of five means, b'_{ijr} , about their mean b'_{ij} .

There is an additional component of random uncertainty due to the rescaling of the CDGs to the RSGs due to the random noise exhibited at 100 Pa. Therefore, for pressure below 100 Pa, the Type A evaluation of uncertainty for $p_t \leq 100$ Pa is:

$$u_{rdm}(b'_{ij}) = \sqrt{\left(\frac{\sigma_{ijk}}{\sqrt{5}}\right)^2 + u_{rdm}(b'_{CDGij}(100))^2 + u_{rdm}(b'_{RSGij}(100))^2 + u_{lts}(b'_{RSGij}(100))^2} \quad (16).$$

Long-term shifts in gauge response are a significant component of uncertainty, particularly for CDGs, but it is the most difficult to evaluate. This is due to the limited number of repeat calibrations against the same standard and the unknown effect of transportation between laboratories (rough handling, large temperature changes, etc.). Earlier studies at the pilot laboratory [3,19] have shown that changes in response functions of CDGs and RSGs between calibrations generally do not occur as a monotonic drift with time (over intervals of months to years) but rather as shifts that are essentially random in both sign and magnitude. Furthermore, the earlier studies showed that, at least for low range CDGs, the magnitude of the shifts was on average about a factor of two larger for gauges transported between laboratories than for gauges maintained at the pilot laboratory.

An evaluation of sensor health was done by comparing the primary transfer package (pkg B), that was shipped to each participant, to a package that remained at the pilot laboratory (pkg A). Figure 8 and 9 shows the CDG's and RSG's calibration ratios for gauge 2 plotted against those for gauge 1 in each package. The data corresponds to calibration ratios at each target pressure for the three repeat calibrations at the pilot laboratory. For the CDGs shown in Figure 8, the drift in scale and direction appears random and similar between the two packages. The RSGs show similar results, however as the drift is much lower, the point distribution looks random and patterns are hard to discern. From this data we can ascertain that the sensors returned in good health and that the drift throughout the comparison was random and not caused by one event/shock.

Assuming the observed variability in gauge response was purely random and taking into account the small statistical sample of pilot laboratory calibrations (three), a Type B evaluation was used to estimate the uncertainty $u_{lts}(b'_{ij})$ for each gauge. At each target pressure, the variation due to long-term shifts was modeled by a normal distribution such that there is a 2 out of 3 chance the calibration ratio lies in the interval between maximum and minimum values of b'_{ij} measured during the three calibrations at the pilot laboratory. Then the standard uncertainty due to this source of error equals one-half the difference between the maximum and minimum values:

$$u_{lts}(b'_{ij}) = \frac{(b'_{NISTi})_{max} - (b'_{NISTi})_{min}}{2} \quad (17).$$

This estimate is unaffected by any systematic bias in the pilot laboratory standard, which would be present in all three calibrations. However, the estimate does assume stability in the laboratory standard at the pilot laboratory and that the observed shifts are attributed to gauges instability.

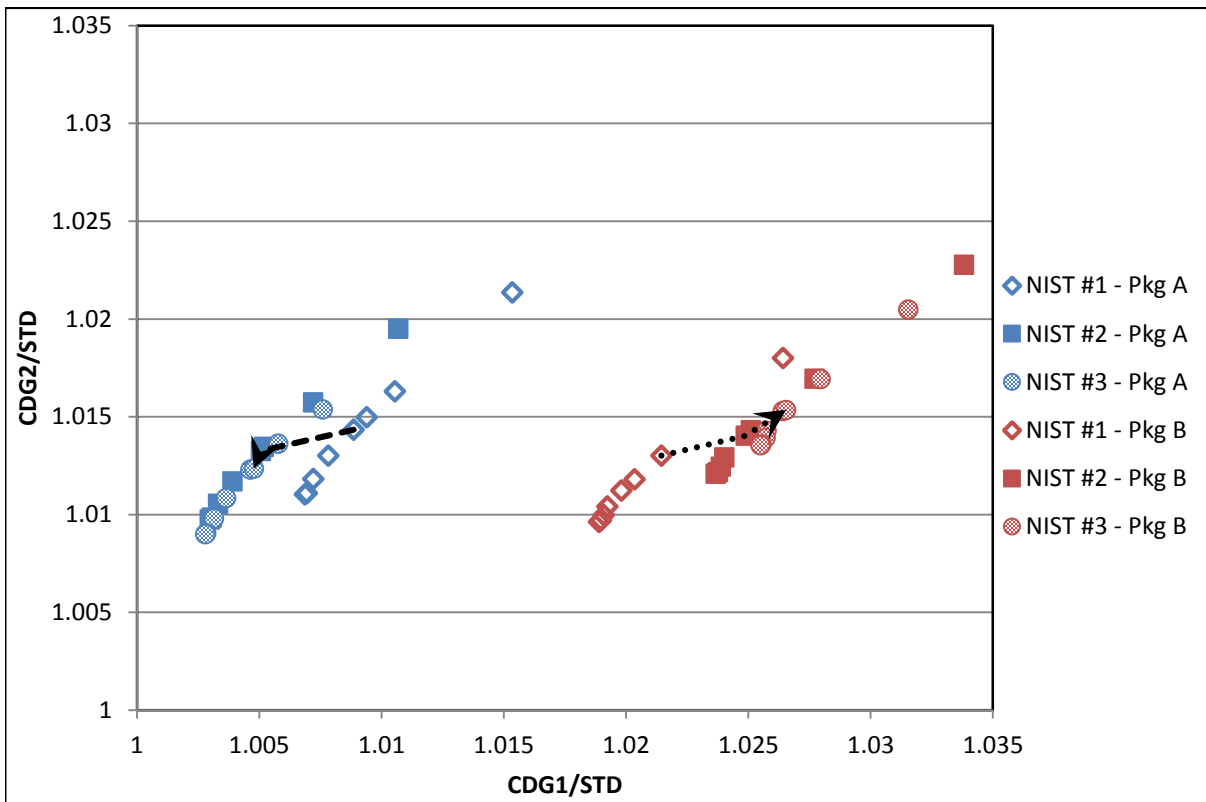


Figure 8. Long term instability of CDG Calibration ratios as measured at pilot laboratory. Individual points refer to data at different target pressures and dashed lines show progression.

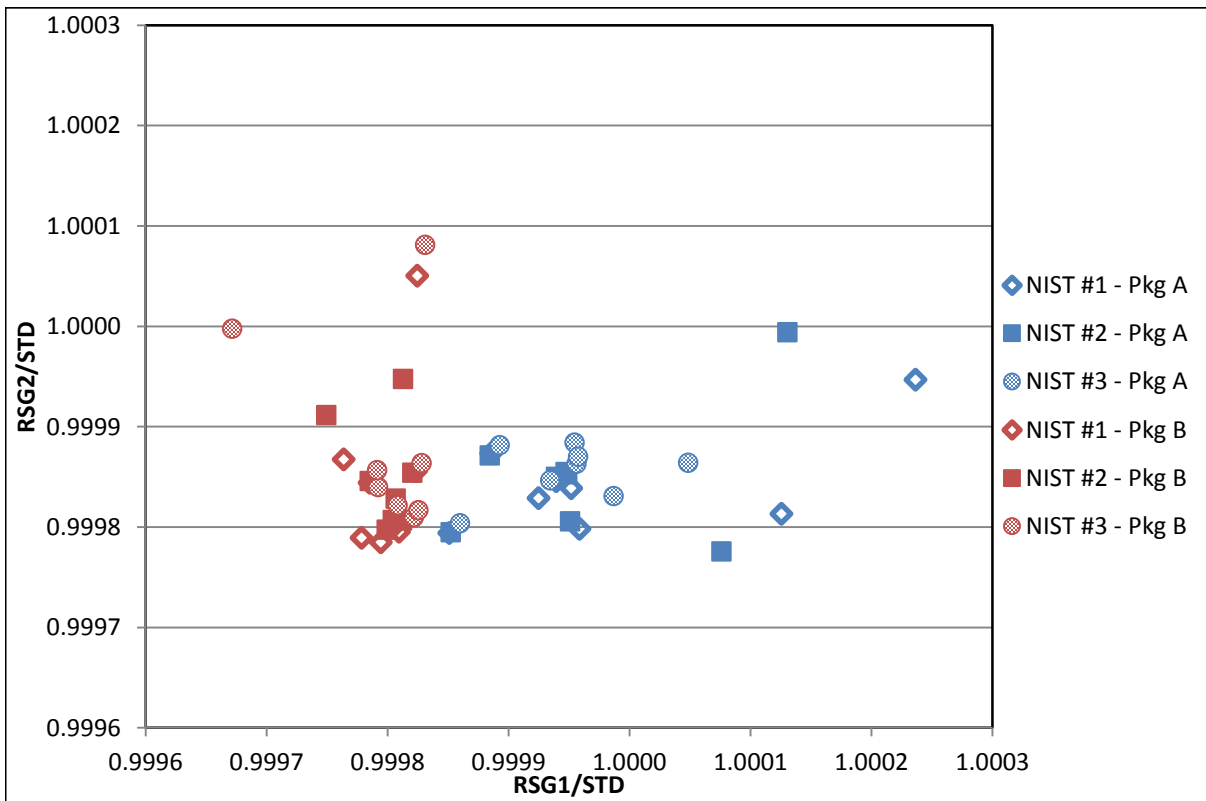


Figure 9. Long term instability of RSG Calibration ratios as measured at pilot laboratory. Individual points refer to data at different target pressures.

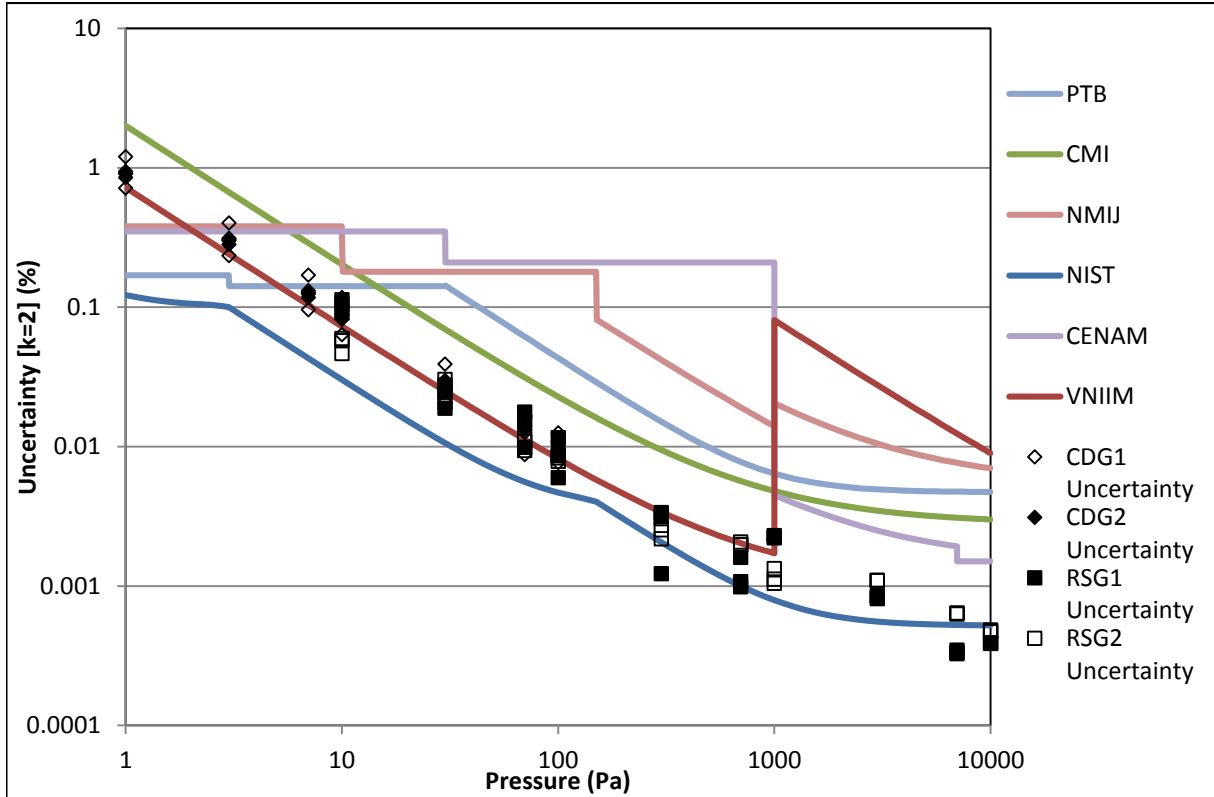


Figure 10. Transfer standard relative uncertainty superimposed on relative uncertainties of the laboratory standards.

Figure 10 shows the relative uncertainties of the transfer standard gauge readings superimposed upon

the relative uncertainties of the laboratory standards. From this it is evident that the uncertainty of the transfer standard has the same order of magnitude or smaller uncertainty than the laboratory standards at the NMIs. This plot shows that the long-term stability of the transfer standard over the course of this comparison should be sufficient to resolve any relative biases between different laboratory standards.

Table 2. Long term instability of CDG Calibration ratios as measured at pilot laboratory.

	$U_{lts}(b_{ij})$ (Pa)			
	CDG1	CDG2	RSG1	RSG2
1	0.0020	0.0018		
3	0.0023	0.0021		
10	0.0015	0.0015	0.0089	0.0016
30	0.0017	0.0006	0.0036	0.0054
100	0.0046	0.0065	0.0046	0.0065
300			0.0022	0.0060
1000			0.0217	0.0102
3000			0.0237	0.0325
7000			0.0224	0.0437
10000			0.0380	0.0469

The combined uncertainty in the normalized gauge readings, p_{ij} , at each target pressure was estimated by using data from Tables 2 and 4,

and Equations (12) to (14), and is given in Table 4.

6.7. ESTIMATES OF UNCERTAINTIES IN THE CORRECTED MEAN GAUGE READINGS

The combined gauge reading p_j , of CDG1 and CDG2 or RSG1 and RSG2 as calculated via Equation (10), requires the uncertainties of the corrected mean gauge reading $u_c(p_j)$ be calculated using the following equation:

$$u_c(p_j) = \sqrt{u_{std}(p_j)^2 + \sum_{i=1}^2 c_1^2 u_{rdm}(p_{ij})^2 + \sum_{i=1}^2 c_2^2 u_{lts}(p_{ij})^2} \quad (18),$$

where $u_{std}(p_j)$ is the uncertainty for the NMI's standard, $c_1 = c_2 = 1/2$ is the (common) value for the partial derivatives $(\partial p_j / \partial p_{ij})$ of Equation (9). Equation (18) is only valid for the non-pilot laboratories.

For the pilot laboratory, $\langle p_j \rangle_n$ is the mean of twelve values of p_{ij} , where n is the calibration number 1, 2, 3 (see discussion following Equation (17)). In this case the combined uncertainty in p_j was estimated from:

$$u_c(p_j) = \sqrt{u_{std}(p_j)^2 + \sum_{n=1}^3 \sum_{i=1}^2 c_1^2 u_{rdm}(p_{ijn})^2 + \sum_{i=1}^2 c_2^2 u_{lts}(p_{ij})^2} \quad (19),$$

where $c_1 = 1/6$ and $c_2 = 1/2$ and $j = \text{pilot (NIST)}$. Note that the multiple calibrations tend to reduce the influence of uncorrelated uncertainties arising from short-term variability of the gauges on the combined uncertainty in p_j .

6.8. EVALUATION OF DEGREES OF EQUIVALENCE

The Mutual Recognition Arrangement (MRA) [22] proposes that the equivalence of a NMI laboratory standard may be stated in two ways, equivalence relative to a key comparison reference value (KCRV) and equivalence between pairs of national standards. Several procedures can be used to define a KCRV each having both advantages and disadvantages and the reader is referred to reference [1] for a discussion of the benefits and drawbacks of different approaches. The proposed definition of a KCRV at each target pressure is calculated by an unweighted mean of the measured values. This method was selected as a reasonable procedure to obtain reference values for this key comparison because this method is similar to that used in the previous CCM.P-K4 [1] and additionally, it was determined to provide an equal chance for all labs to factor into the comparison value. Using this method the KCRV is calculated by

$$p_{KCRV} = \frac{1}{N} \sum_j^N p_j \quad (20).$$

The degree of equivalence of laboratory standard j relative to a KCRV is expressed at each target pressure by two quantities, the deviation of p_j from the reference value p_{KCRV}

$$D_j = p_j - p_{KCRV} \quad (21)$$

and the expanded uncertainty of this deviation, which is estimated from

$$U_j = k u_c(D_j) = k \sqrt{\left(1 - \frac{2}{N}\right) u_c(p_j)^2 + \frac{1}{N^2} \sum_j^N u_c(p_j)^2} \quad (22),$$

where $u_c(D_j)$ is the combined standard uncertainty of this deviation, k is the coverage factor ($k = 2$ was used to represent the expanded uncertainty), $u_c(p_j)$ is the combined uncertainties in the corrected mean gauge readings given by Equations (18) or (19), and N is equal to the number of participating laboratory standards j at each pressure.

Following the definition given in the MRA, the degree of equivalence between pairs of laboratory standards j and j' may be expressed at each target pressure by two quantities, the difference of their deviations from the reference value⁴

$$D_{jj'} = D_j - D_{j'} = (p_j - p_{KCRV}) - (p_{j'} - p_{KCRV}) = p_j - p_{j'} \quad (23)$$

and the expanded uncertainty of this difference, which is estimated from

$$U_{jj'} = ku_c(D_{jj'}) = k\sqrt{u_c(p_j)^2 + u_c(p_{j'})^2} \quad (24),$$

where $u_c(D_{jj'})$ is the combined standard uncertainty of this difference, k is the coverage factor ($k = 2$ was used to represent the expanded uncertainty), $u_c(p_j)$ and $u_c(p_{j'})$ are the combined uncertainties in the corrected mean gauge readings obtained with laboratory standards j and j' , respectively, which are estimated from Equation (18) or (19).

7. RESULTS FOR KEY COMPARISON CCM.P-K4

7.1. COMPARISON OF NORMALIZED GAUGE READINGS

Table 3 presents a summary of the normalized gauge readings, p_{ij} , obtained from the participating laboratories as a function of nominal target pressures. The calibration ratios for the CDGs after re-scaling to the RSGs, were calculated using Equations (6b), and are given in column three and four. The ratios for the RSGs calculated via Equation (4) are given in column five and six. Values of p'_{ij} , which were calculated via Equation (9), are given in columns seven through ten. Column eleven is the combined CDG or RSG reading p_j and calculated by Equation (10) or (11).

Table 4 summarizes the uncertainty calculations for the participating laboratories as a function of pressure. Uncertainties in the ratios due to Type A effects, which were obtained by means of Equation (15) or (16), are given in columns three through six. The combined standard uncertainties, $u_c(p_{ij})$, which were calculated according to Equation (12), are given in column seven through ten. Column eleven is the combined uncertainty, $u_c(p_j)$ as calculated by Equation (18) or (19).

The results for the normalized gauge readings, p'_{ij} , and their standard ($k = 1$) uncertainties, $u_c(p'_{ij})$, are presented in Figures 11 through 20 in the form of Youden plots [25] in which the difference $p'_{2j} - p_t$ is plotted as a function of $p'_{1j} - p_t$. The y - and x -axes can be described as the difference between gauge reading and the standard at each NMI (normalized to the target pressure).

Youden plots are particularly useful for graphical representation and interpretation of key comparison results obtained with pairs of transfer artifacts. If only random errors of precision are present the data points from individual laboratory standards will be distributed in a circular/ball shape pattern (in the limit of a large number of standards). However if there is relative bias between individual standards the data points will be distributed along a diagonal at 45 degrees to the positive y - and x -axes because standards that measure/generate pressures low (or high) relative to one gauge will do the same relative to the second gauge. The scatter of data in a direction perpendicular to this diagonal provides a measure of precision of the transfer standard gauges. The Youden plots of the present results clearly show that the transfer standards have sufficient precision to differentiate relative systematic biases between individual laboratory standards.

⁴ The statement of equivalence between pairs of standards is written as stated in the mutual recognition agreement [22], but in reality the difference $D_{jj'}$ does not require the calculation of a KCRV.

Table 3. Summary of key comparison results for measured/rescaled calibration ratios, b_{ij} , and calculated values for normalized readings of gauge i , p'_{ij} , at the target pressure, and the mean gauge reading p_j .

NMI	Nominal Pressure (Pa)	Rescaled CDG Ratios		RSG Ratios		Normalized Gauge Reading (Pa)				Mean Reading (Pa) p_j
		CDG1 b_{ij}	CDG2 b_{ij}	RSG1 b_{ij}	RSG2 b_{ij}	CDG1 p'_{ij}	CDG2 p'_{ij}	RSG1 p'_{ij}	RSG2 p'_{ij}	
PTB	1	1.0010	1.0022			1.0010	1.0022			1.0016
	3	1.0008	1.0019			3.0025	3.0058			3.0042
	10	1.0002	1.0011			10.0024	10.0110			10.0067
	30	0.9999	1.0005			29.9959	30.0137			30.0048
	100	0.9999	1.0000	0.9999	1.0000	99.9883	99.9996	99.9883	99.9996	99.9939
	300			0.9998	0.9999			299.9355	299.9572	299.9463
	1000			0.9998	0.9998			999.8414	999.8211	999.8313
	3000			0.9999	0.9998			2999.5815	2999.5421	2999.5618
	7000			0.9998	0.9999			6998.7411	6999.1440	6998.9425
	10000			0.9998	0.9999			9998.4197	9998.7355	9998.5776
CMI	1	1.0041	1.0053			1.0041	1.0053			1.0047
	3	1.0050	1.0061			3.0150	3.0184			3.0167
	10	1.0026	1.0036			10.0259	10.0362			10.0311
	30	1.0009	1.0017			30.0276	30.0503			30.0390
	100	1.0000	1.0003	1.0000	1.0003	100.0022	100.0281	100.0022	100.0281	100.0151
	300			0.9999	0.9999			299.9594	299.9752	299.9673
	1000			0.9998	0.9999			999.8470	999.8544	999.8507
	3000			0.9999	0.9998			2999.5525	2999.5259	2999.5392
	7000			0.9998	0.9999			6998.7429	6999.1655	6998.9542
	10000			0.9999	0.9999			9998.5588	9998.8969	9998.7279
NMIJ	1	1.0020	1.0028			1.0020	1.0028			1.0024
	3	1.0013	1.0023			3.0040	3.0070			3.0055
	10	1.0003	1.0012			10.0028	10.0125			10.0076
	30	0.9997	1.0004			29.9904	30.0108			30.0006
	100	0.9995	0.9997	0.9995	0.9997	99.9505	99.9661	99.9505	99.9661	99.9583
	300			0.9997	0.9998			299.9139	299.9288	299.9213
	1000			0.9998	0.9998			999.8016	999.8035	999.8025
	3000			0.9998	0.9998			2999.4902	2999.4562	2999.4732
	7000			0.9998	0.9999			6998.6637	6999.0866	6998.8751
	10000			0.9998	0.9999			9998.4318	9998.7793	9998.6056
NIST Avg	1	1.0075	1.0085			1.0075	1.0085			1.0080
	3	1.0027	1.0038			3.0081	3.0113			3.0097
	10	1.0008	1.0017			10.0078	10.0170			10.0124
	30	1.0000	1.0007			30.0014	30.0215			30.0115
	100	0.9998	1.0000	0.9998	1.0000	99.9823	100.0026	99.9823	100.0026	99.9925
	300			0.9998	0.9998			299.9403	299.9468	299.9435
	1000			0.9998	0.9998			999.7998	999.7988	999.7993
	3000			0.9998	0.9998			2999.4469	2999.4192	2999.4330
	7000			0.9998	0.9998			6998.5106	6998.9425	6998.7265
	10000			0.9998	0.9999			9998.2402	9998.5790	9998.4096
CENAM	1	0.9909	0.9923			0.9909	0.9923			0.9916
	3	0.9957	0.9969			2.9870	2.9907			2.9888
	10	0.9954	0.9964			9.9544	9.9642			9.9593
	30	0.9953	0.9960			29.8583	29.8799			29.8691
	100	0.9981	0.9983	0.9981	0.9983	99.8051	99.8289	99.8051	99.8289	99.8170
	300			0.9992	0.9993			299.7722	299.7924	299.7823
	1000			0.9995	0.9995			999.4905	999.5045	999.4975
	3000			0.9998	0.9998			2999.5177	2999.5004	2999.5090
	7000			0.9998	0.9999			6998.5196	6998.9520	6998.7358
	10000			0.9998	0.9999			9998.2116	9998.5747	9998.3932
VNIIM	1	1.0000	1.0019			1.0000	1.0019			1.0010
	3	0.9990	1.0004			2.9970	3.0011			2.9990
	10	0.9995	1.0005			9.9949	10.0050			10.0000
	30	0.9996	1.0003			29.9883	30.0083			29.9983
	100	0.9994	0.9996	0.9994	0.9996	99.9428	99.9584	99.9428	99.9584	99.9506
	300			0.9995	0.9996			299.8634	299.8670	299.8652
	1000			0.9996	0.9996			999.5699	999.5766	999.5732
	3000			0.9999	0.9999			2999.8082	2999.7896	2999.7989
	7000			0.9999	0.9999			6998.9513	6999.4085	6999.1799
	10000			0.9999	0.9999			9998.7350	9999.0907	9998.9129

Table 4. Summary of key comparison uncertainties due to random effects, $u_{rdm}(b_{ij})$, the combined uncertainty $u_c(p_{ij})$, and the uncertainty of the mean gauge reading $u_c(p_j)$.

NMI	Nominal Pressure (Pa)	$u_{rdm}(b_{ij})$ (Pa)				$u_c(p_{ij})$ (Pa)				$u_c(p_j)$ (Pa)
		CDG1	CDG2	RSG1	RSG2	CDG1	CDG2	RSG1	RSG2	
PTB	1	0.0074	0.0087			0.0077	0.0089			0.0043
	3	0.0074	0.0087			0.0081	0.0093			0.0050
	10	0.0074	0.0087			0.0106	0.0116			0.0086
	30	0.0074	0.0087			0.0233	0.0237			0.0224
	100	0.0079	0.0093	0.0049	0.0045	0.0238	0.0248	0.0230	0.0234	0.0226
	300			0.0125	0.0112			0.0263	0.0263	0.0247
	1000			0.0066	0.0094			0.0392	0.0349	0.0346
	3000			0.0076	0.0090			0.0781	0.0813	0.0769
	7000			0.0038	0.0031			0.1715	0.1756	0.1718
	10000			0.0185	0.0174			0.2437	0.2451	0.2422
CMI	1	0.0203	0.0234			0.0228	0.0255			0.0181
	3	0.0204	0.0234			0.0228	0.0255			0.0181
	10	0.0204	0.0234			0.0228	0.0255			0.0181
	30	0.0203	0.0234			0.0229	0.0256			0.0183
	100	0.0205	0.0235	0.0196	0.0222	0.0239	0.0269	0.0231	0.0258	0.0191
	300			0.0194	0.0231			0.0242	0.0278	0.0210
	1000			0.0205	0.0220			0.0383	0.0341	0.0307
	3000			0.0166	0.0242			0.0595	0.0659	0.0576
	7000			0.0201	0.0254			0.1121	0.1193	0.1119
	10000			0.0199	0.0217			0.1560	0.1587	0.1537
NMIJ	1	0.0090	0.0087			0.0092	0.0090			0.0051
	3	0.0090	0.0088			0.0096	0.0094			0.0058
	10	0.0090	0.0088			0.0128	0.0126			0.0274
	30	0.0090	0.0088			0.0285	0.0284			0.0801
	100	0.0090	0.0088	0.0076	0.0058	0.0906	0.0907	0.0904	0.0904	0.0902
	300			0.0063	0.0033			0.0803	0.0803	0.0801
	1000			0.0114	0.0065			0.0933	0.0908	0.0910
	3000			0.0141	0.0109			0.1624	0.1636	0.1615
	7000			0.0169	0.0163			0.2715	0.2740	0.2714
	10000			0.0154	0.0095			0.3524	0.3533	0.3514
NIST Avg	1	0.0093	0.0088			0.0096	0.0090			0.0033
	3	0.0092	0.0086			0.0096	0.0090			0.0036
	10	0.0089	0.0084			0.0092	0.0087			0.0033
	30	0.0088	0.0084			0.0091	0.0085			0.0033
	100	0.0089	0.0084	0.0073	0.0051	0.0103	0.0109	0.0091	0.0086	0.0057
	300			0.0073	0.0047			0.0084	0.0084	0.0052
	1000			0.0063	0.0051			0.0230	0.0123	0.0129
	3000			0.0076	0.0052			0.0263	0.0339	0.0219
	7000			0.0071	0.0080			0.0299	0.0481	0.0309
	10000			0.0088	0.0074			0.0470	0.0543	0.0401
CENAM	1	0.0203	0.0186			0.0204	0.0188			0.0139
	3	0.0202	0.0186			0.0210	0.0195			0.0148
	10	0.0204	0.0187			0.0281	0.0269			0.0237
	30	0.0218	0.0201			0.0564	0.0558			0.0541
	100	0.0227	0.0214	0.0167	0.0138	0.1076	0.1074	0.1065	0.1062	0.1057
	300			0.0086	0.0107			0.3160	0.3162	0.3160
	1000			0.0195	0.0168			1.0682	1.0680	1.0679
	3000			0.0499	0.0452			0.0738	0.0741	0.0627
	7000			0.0769	0.0667			0.1012	0.1009	0.0838
	10000			0.0422	0.0404			0.0996	0.1026	0.0920
VNIIM	1	0.0202	0.0186			0.0206	0.0190			0.0137
	3	0.0203	0.0187			0.0208	0.0192			0.0138
	10	0.0204	0.0188			0.0208	0.0193			0.0139
	30	0.0204	0.0188			0.0211	0.0195			0.0143
	100	0.0227	0.0214	0.0167	0.0138	0.0247	0.0240	0.0193	0.0175	0.0144
	300			0.0054	0.0029			0.0195	0.0198	0.0191
	1000			0.0180	0.0168			0.0606	0.0571	0.0563
	3000			0.0695	0.0701			0.4727	0.4734	0.4700
	7000			0.0648	0.0615			0.4908	0.4918	0.4887
	10000			0.0716	0.0697			0.5075	0.5080	0.5044

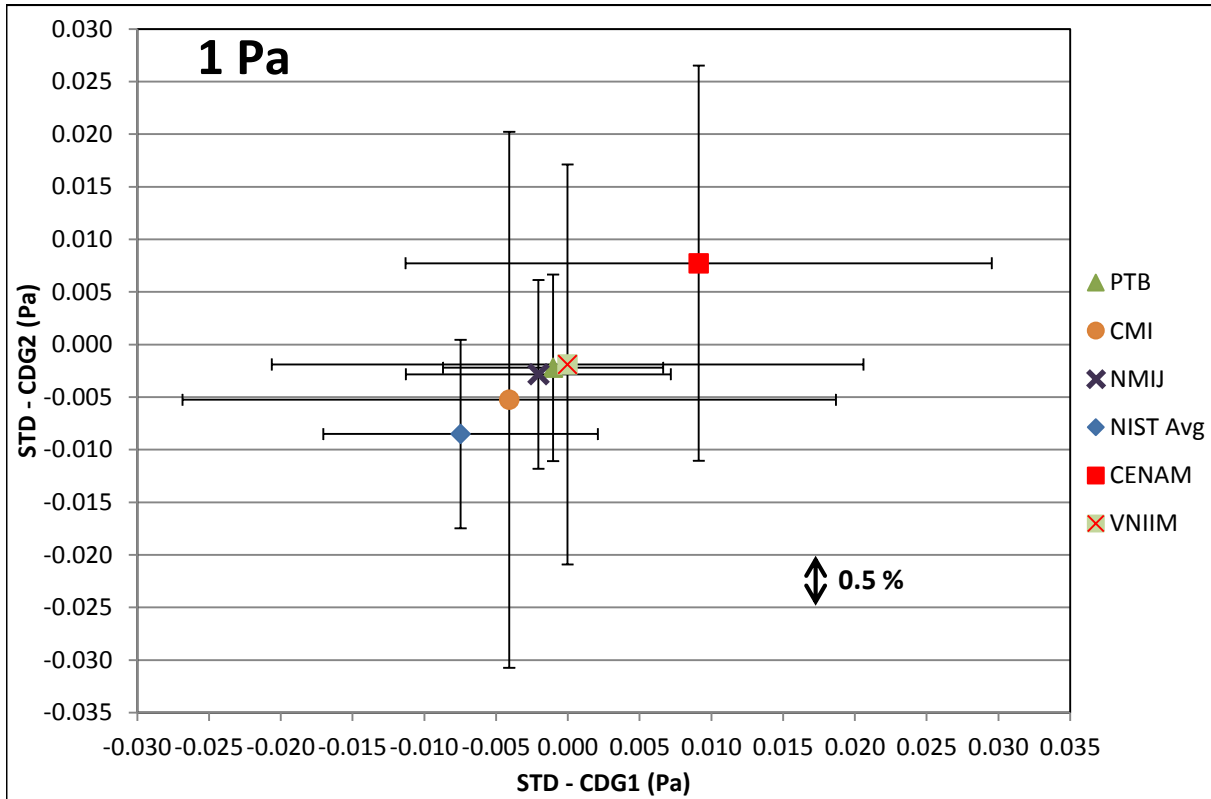


Figure 11. Youden plot of differences between normalized pressure readings of CDGs and pressures measured/generated by laboratory standards when equal to target pressures of 1 Pa. Uncertainty bars refer to combined standard ($k = 1$) uncertainties.

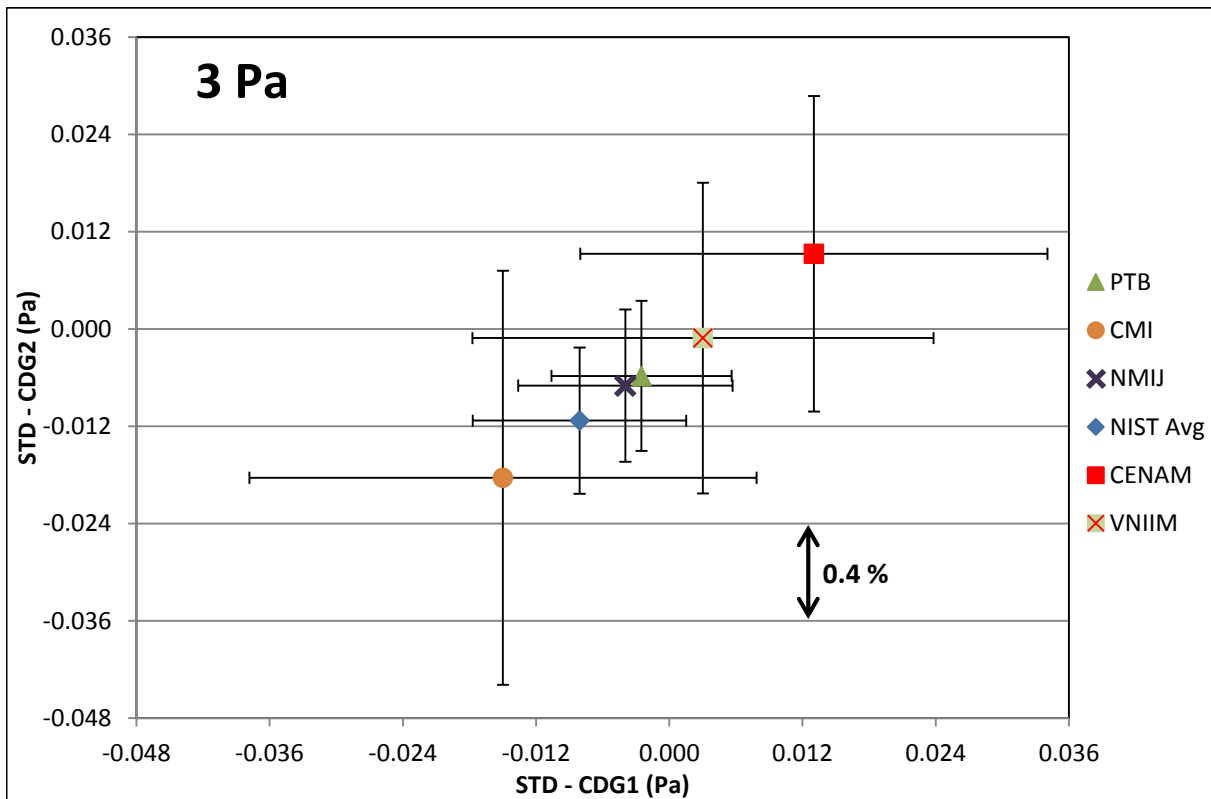


Figure 12. Youden plot of differences between normalized pressure readings of CDGs and pressures measured/generated by laboratory standards when equal to target pressures of 3 Pa. Uncertainty bars refer to combined standard ($k = 1$) uncertainties.

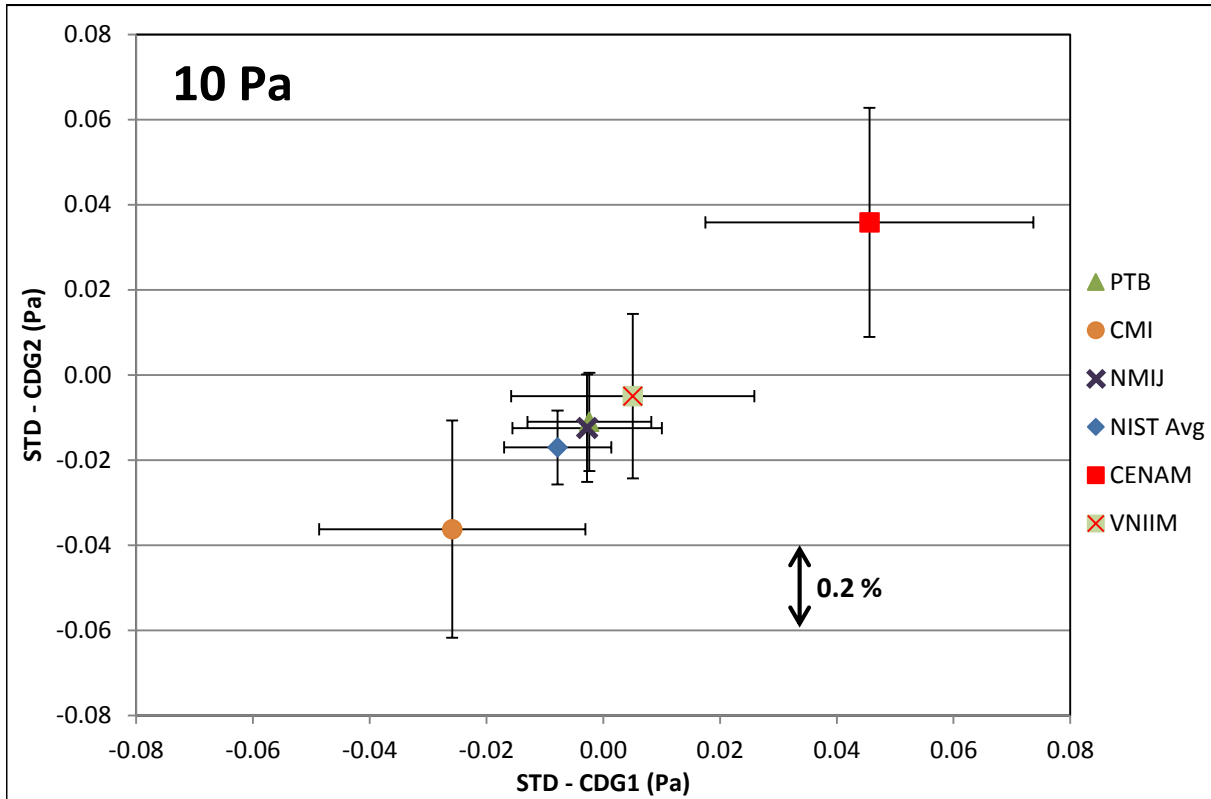


Figure 13. Youden plot of differences between normalized pressure readings of CDGs and pressures measured/generated by laboratory standards when equal to target pressures of 10 Pa. Uncertainty bars refer to combined standard ($k = 1$) uncertainties.

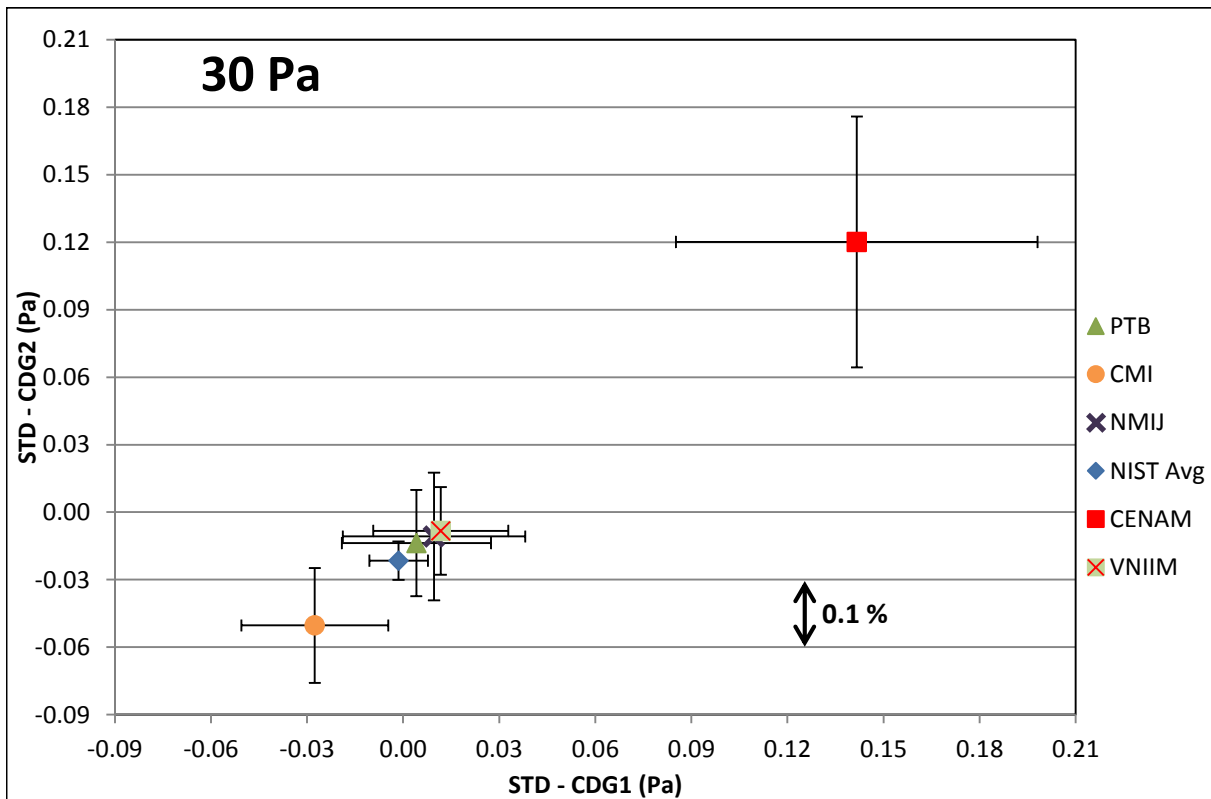


Figure 14. Youden plot of differences between normalized pressure readings of CDGs and pressures measured/generated by laboratory standards when equal to target pressures of 30 Pa. Uncertainty bars refer to combined standard ($k = 1$) uncertainties.

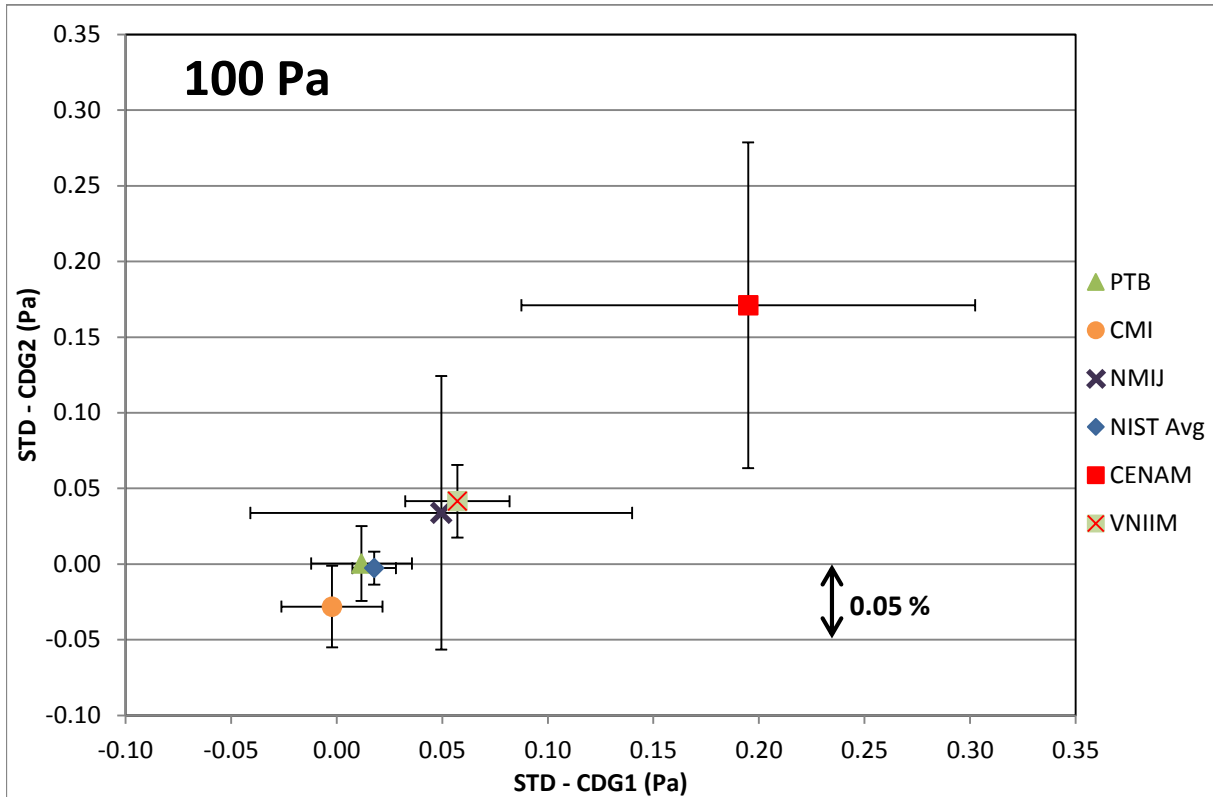


Figure 15. Youden plot of differences between normalized pressure readings of RSGs and pressures measured/generated by laboratory standards when equal to target pressures of 100 Pa. Uncertainty bars refer to combined standard ($k = 1$) uncertainties.

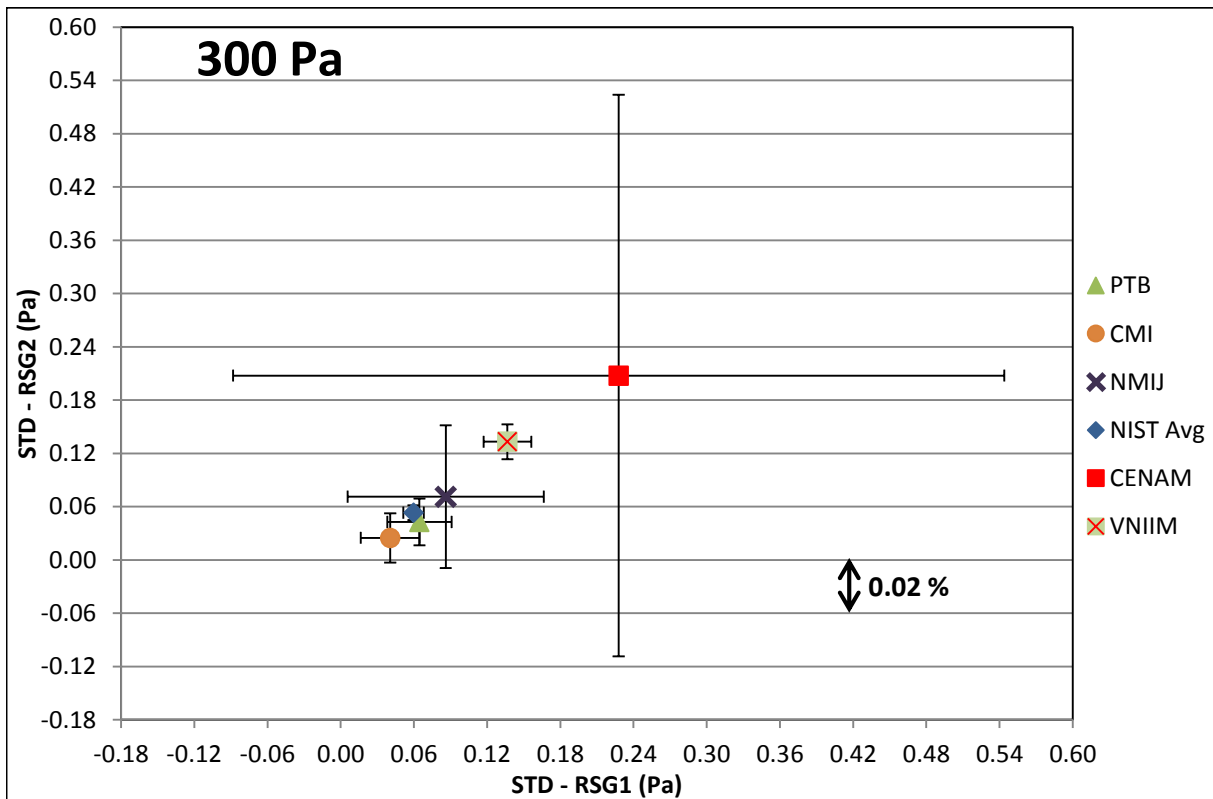


Figure 16. Youden plot of differences between normalized pressure readings of RSGs and pressures measured/generated by laboratory standards when equal to target pressures of 300 Pa. Uncertainty bars refer to combined standard ($k = 1$) uncertainties.

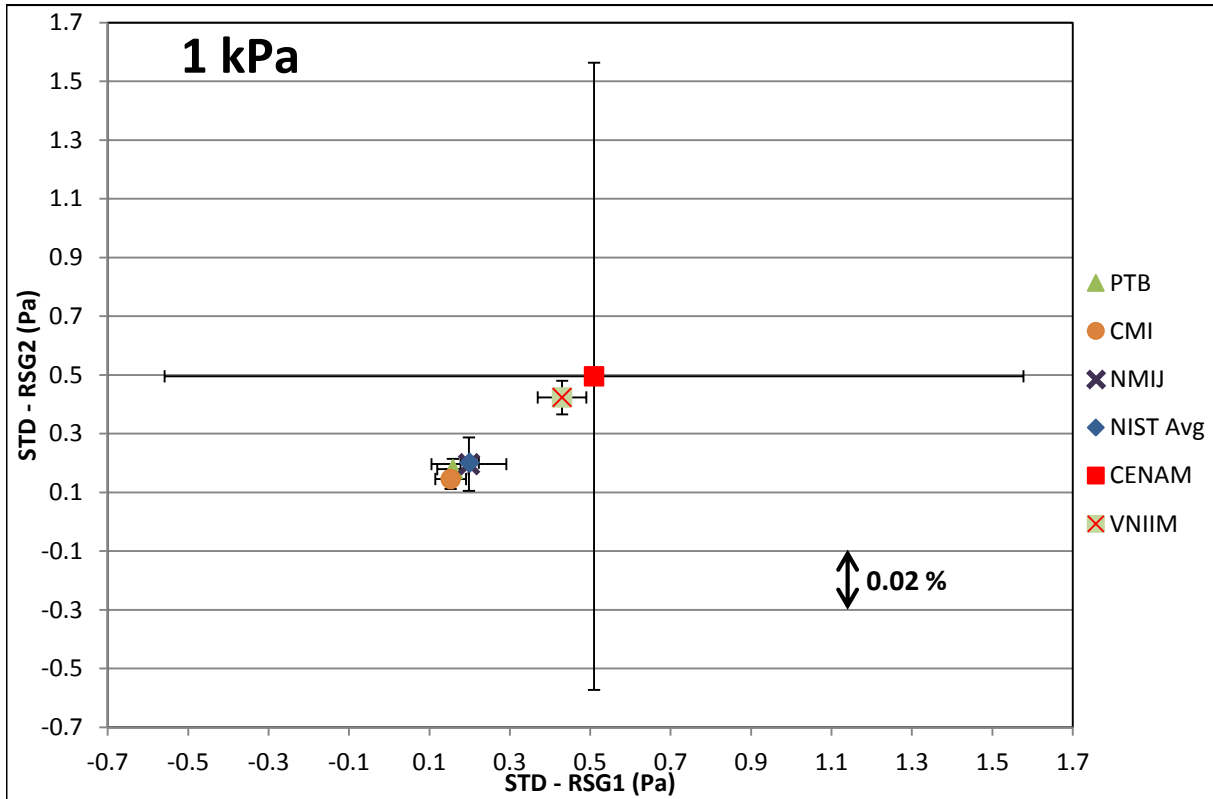


Figure 17. Youden plot of differences between normalized pressure readings of RSGs and pressures measured/generated by laboratory standards when equal to target pressures of 1000 Pa. Uncertainty bars refer to combined standard ($k = 1$) uncertainties.

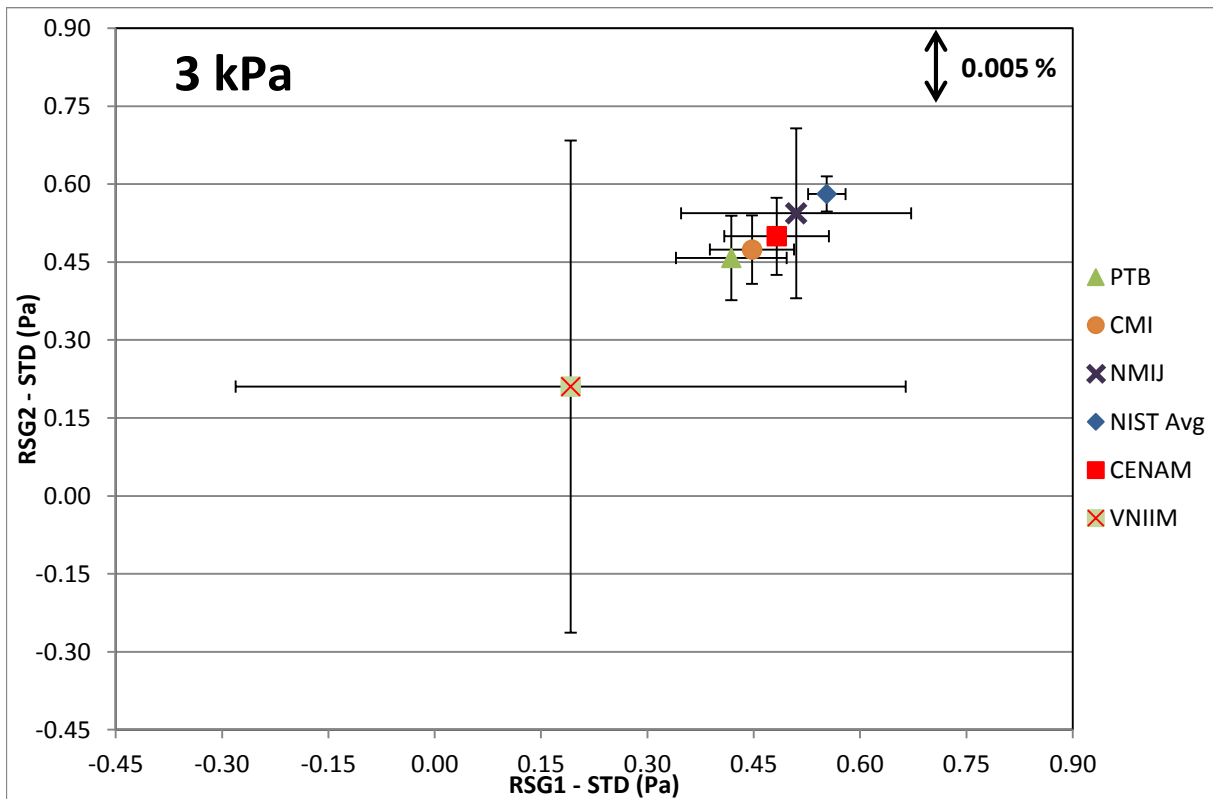


Figure 18. Youden plot of differences between normalized pressure readings of RSGs and pressures measured/generated by laboratory standards when equal to target pressures of 3000 Pa. Uncertainty bars refer to combined standard ($k = 1$) uncertainties.

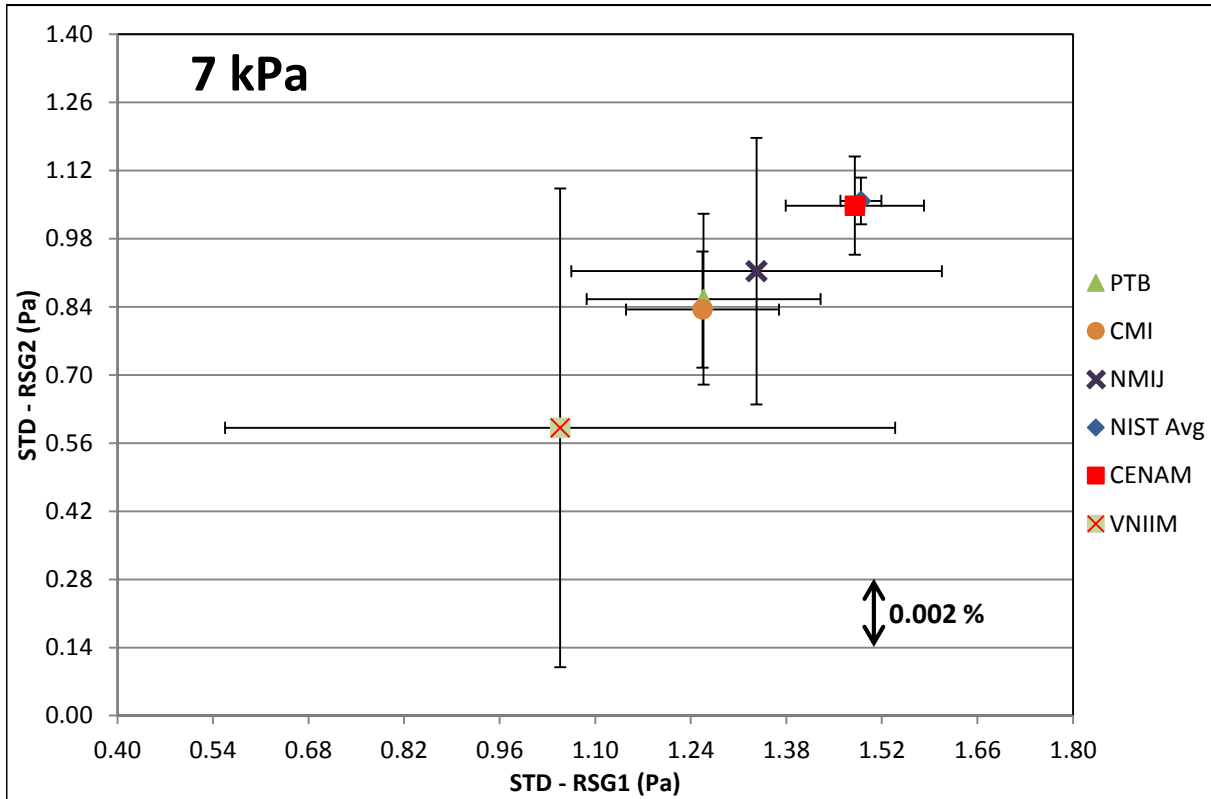


Figure 19. Youden plot of differences between normalized pressure readings of RSGs and pressures measured/generated by laboratory standards when equal to target pressures of 7000 Pa. Uncertainty bars refer to combined standard ($k = 1$) uncertainties.

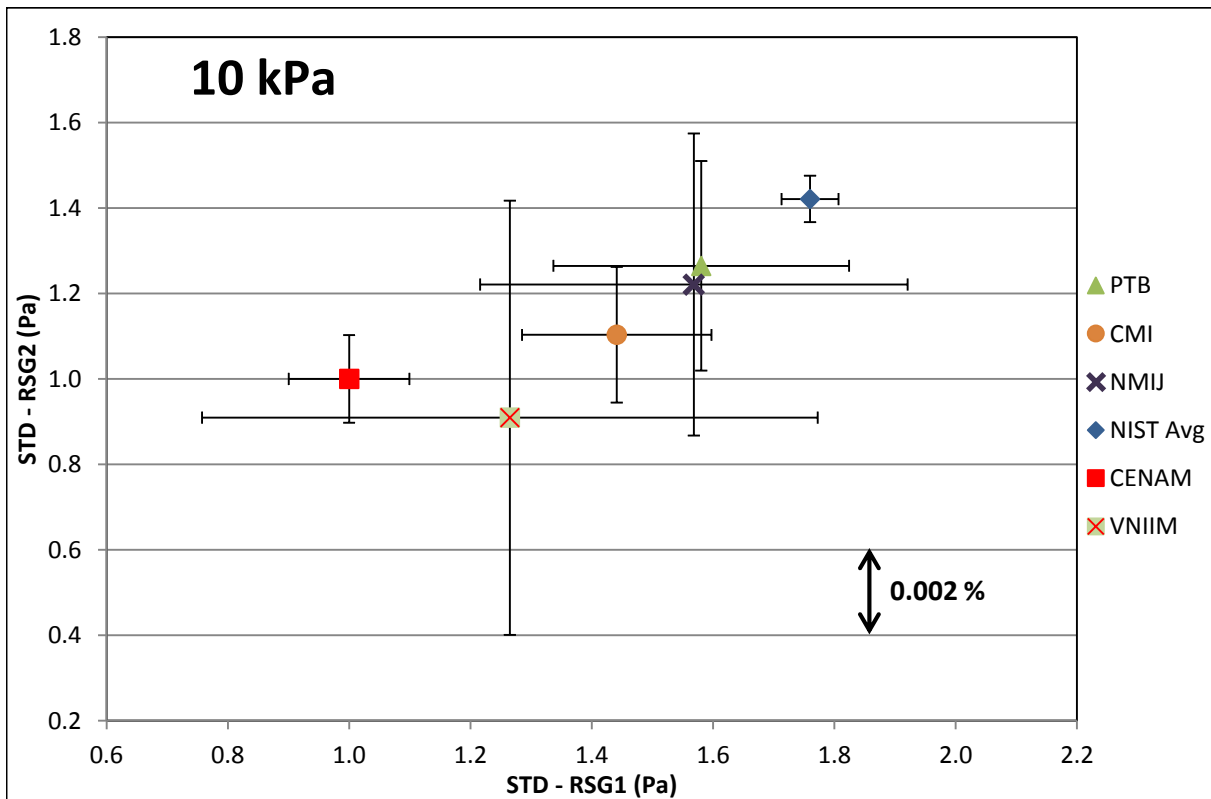


Figure 20. Youden plot of differences between normalized pressure readings of RSGs and pressures measured/generated by laboratory standards when equal to target pressures of 10000 Pa. Uncertainty bars refer to combined standard ($k = 1$) uncertainties.

7.2. DEGREES OF EQUIVALENCE OF THE LABORATORY STANDARDS

The values for the corrected mean gauge readings p_j , which were calculated from Equation (10) or (11), and the combined uncertainties $u_c(p_j)$, which were calculated using Equation (18) or (19), are given in Tables 3 and 4, respectively. These values are used to compare the results of the comparison. Table 5 presents a summary of final results for the participant NMIs as a function of nominal target pressures. The columns present degrees of equivalence of the measurement standards expressed quantitatively in two ways: deviations from KCRV and pairwise differences between each NMI. The deviations from KCRV, D_j , were calculated via Equation (20). The expanded uncertainties of these deviations, U_j , were calculated using Equation (21). The pairwise differences between the deviations $D_{jj'}$ and the expanded uncertainties of these differences, $U_{jj'}$, were calculated using Equations (23) and (24). The red shaded cells in Table 5 indicate pressures at which the condition for equivalence at the $k = 2$ level of confidence is not satisfied, that is, where $|D_j| > U_j$ or $|D_{jj'}| > U_{jj'}$.

When interpreting the results in Table 5 it is important to note that the pairwise difference may be regarded as a surrogate for the difference in “true” pressures actually realized by the pair of laboratory standards when they are set to measure/generate the same target pressure. Similarly, D_j represents the deviation of the “true” pressure realized by laboratory standard j from the corresponding key comparison reference value. D_j is not necessarily equal to the deviation of laboratory standard j from the SI value. Although the key comparison reference value is likely to be a close approximation to the SI value, it is just used for comparison purposes and not for the definition/realization of the SI unit of Pascal.

The degrees of equivalence of individual NMIs with respect to key comparison reference values are presented graphically in Figures 21 to 30 as plots of deviations, D_j , versus NMI. Uncertainty bars are the values of U_j , at the $k = 2$ confidence interval.

Table 5. Degrees of equivalence expressed in two ways, equivalence of NMIs relative to key comparison reference values, and equivalence between pairs of NMIs. The shaded cells indicate apparent nonequivalence of results for which $|D_j|$ exceeds U_j or $|D_{jj}|$ exceeds U_{jj} .

NMI	Target Pressure (Pa)	KCRV		PTB		CMI		NMIJ		NIST		CENAM		VNIIM	
		D_j	U_j	D_{jj}	U_{jj}										
PTB	1	0.000	0.014												
PTB	3	0.000	0.014												
PTB	10	0.004	0.021												
PTB	30	0.018	0.050												
PTB	100	0.039	0.053												
PTB	300	0.042	0.117												
PTB	1000	0.106	0.363												
PTB	3000	0.01	0.21												
PTB	7000	0.04	0.34												
PTB	10000	-0.03	0.46												
CMI	1	0.003	0.032	0.003	0.039			0.002	0.039	-0.003	0.038	0.013	0.046	0.004	0.047
CMI	3	0.013	0.032	0.013	0.039			0.011	0.040	0.007	0.038	0.028	0.047	0.018	0.047
CMI	10	0.028	0.034	0.024	0.042			0.023	0.067	0.019	0.038	0.072	0.060	0.031	0.047
CMI	30	0.052	0.046	0.034	0.059			0.038	0.165	0.027	0.038	0.170	0.114	0.041	0.048
CMI	100	0.061	0.049	0.021	0.059			0.057	0.184	0.023	0.040	0.198	0.215	0.065	0.048
CMI	300	0.063	0.115	0.021	0.065			0.046	0.166	0.024	0.043	0.185	0.633	0.102	0.057
CMI	1000	0.125	0.362	0.019	0.093			0.048	0.192	0.051	0.067	0.353	2.137	0.277	0.128
CMI	3000	-0.01	0.19	-0.02	0.19			0.07	0.34	0.11	0.12	0.03	0.17	-0.26	0.95
CMI	7000	0.05	0.27	0.01	0.41			0.08	0.59	0.23	0.23	0.22	0.28	-0.23	1.00
CMI	10000	0.12	0.34	0.15	0.57			0.12	0.77	0.32	0.32	0.33	0.36	-0.18	1.05
NMIJ	1	0.001	0.014	0.001	0.018	-0.002	0.039			-0.006	0.015	0.011	0.031	0.001	0.031
NMIJ	3	0.001	0.015	0.001	0.019	-0.011	0.040			-0.004	0.016	0.017	0.033	0.006	0.032
NMIJ	10	0.005	0.048	0.001	0.059	-0.023	0.067			-0.005	0.056	0.048	0.073	0.008	0.063
NMIJ	30	0.013	0.135	-0.004	0.167	-0.038	0.165			-0.011	0.160	0.131	0.193	0.002	0.163
NMIJ	100	0.004	0.059	-0.036	0.186	-0.057	0.184			-0.034	0.181	0.141	0.278	0.008	0.183
NMIJ	300	0.017	0.171	-0.025	0.168	-0.046	0.166			-0.022	0.161	0.139	0.652	0.056	0.165
NMIJ	1000	0.077	0.388	-0.029	0.195	-0.048	0.192			0.003	0.184	0.305	2.144	0.229	0.214
NMIJ	3000	-0.08	0.31	-0.09	0.36	-0.07	0.34			0.04	0.33	-0.04	0.35	-0.33	0.99
NMIJ	7000	-0.03	0.49	-0.07	0.64	-0.08	0.59			0.15	0.55	0.14	0.57	-0.30	1.12
NMIJ	10000	0.00	0.62	0.03	0.85	-0.12	0.77			0.20	0.71	0.21	0.73	-0.31	1.23
NIST	1	0.006	0.012	0.006	0.014	0.003	0.038	0.006	0.015			0.016	0.029	0.007	0.030
NIST	3	0.006	0.012	0.006	0.015	-0.007	0.038	0.004	0.016			0.021	0.031	0.011	0.030
NIST	10	0.010	0.016	0.006	0.021	-0.019	0.038	0.005	0.056			0.053	0.048	0.012	0.030
NIST	30	0.024	0.035	0.007	0.046	-0.027	0.038	0.011	0.160			0.142	0.109	0.013	0.031
NIST	100	0.038	0.039	-0.001	0.047	-0.023	0.040	0.034	0.181			0.175	0.212	0.042	0.031
NIST	300	0.039	0.110	-0.003	0.050	-0.024	0.043	0.022	0.161			0.161	0.632	0.078	0.040
NIST	1000	0.074	0.359	-0.032	0.074	-0.051	0.067	-0.003	0.184			0.302	2.136	0.226	0.115
NIST	3000	-0.12	0.17	-0.13	0.16	-0.11	0.12	-0.04	0.33			-0.08	0.13	-0.37	0.94
NIST	7000	-0.18	0.21	-0.22	0.35	-0.23	0.23	-0.15	0.55			-0.01	0.18	-0.45	0.98
NIST	10000	-0.19	0.24	-0.17	0.49	-0.32	0.32	-0.20	0.71			0.02	0.20	-0.50	1.01
CENAM	1	-0.010	0.025	-0.010	0.030	-0.013	0.046	-0.011	0.031	-0.016	0.029			-0.009	0.040
CENAM	3	-0.015	0.026	-0.015	0.032	-0.028	0.047	-0.017	0.033	-0.021	0.031			-0.010	0.041
CENAM	10	-0.044	0.041	-0.047	0.051	-0.072	0.060	-0.048	0.073	-0.053	0.048			-0.041	0.056
CENAM	30	-0.118	0.095	-0.136	0.117	-0.170	0.114	-0.131	0.193	-0.142	0.109			-0.129	0.112
CENAM	100	-0.138	0.177	-0.177	0.216	-0.198	0.215	-0.141	0.278	-0.175	0.212			-0.134	0.213
CENAM	300	-0.122	0.528	-0.164	0.634	-0.185	0.633	-0.139	0.652	-0.161	0.632			-0.083	0.633
CENAM	1000	-0.228	1.780	-0.334	2.137	-0.353	2.137	-0.305	2.144	-0.302	2.136			-0.076	2.139
CENAM	3000	-0.04	0.20	-0.05	0.20	-0.03	0.17	0.04	0.35	0.08	0.13			-0.29	0.95
CENAM	7000	-0.17	0.24	-0.21	0.38	-0.22	0.28	-0.14	0.57	0.01	0.18			-0.44	0.99
CENAM	10000	-0.21	0.27	-0.18	0.52	-0.33	0.36	-0.21	0.73	-0.02	0.20			-0.52	1.03
VNIIM	1	-0.001	0.025	-0.001	0.031	-0.004	0.047	-0.001	0.031	-0.007	0.030	0.009	0.040		
VNIIM	3	-0.005	0.025	-0.005	0.031	-0.018	0.047	-0.006	0.032	-0.011	0.030	0.010	0.041		
VNIIM	10	-0.003	0.028	-0.007	0.035	-0.031	0.047	-0.008	0.063	-0.012	0.030	0.041	0.056		
VNIIM	30	0.011	0.042	-0.007	0.054	-0.041	0.048	-0.002	0.163	-0.013	0.031	0.129	0.112		
VNIIM	100	-0.004	0.045	-0.043	0.054	-0.065	0.048	-0.008	0.183	-0.042	0.031	0.134	0.213		
VNIIM	300	-0.039	0.114	-0.081	0.062	-0.102	0.057	-0.056	0.165	-0.078	0.040	0.083	0.633		
VNIIM	1000	-0.153	0.370	-0.258	0.132	-0.277	0.128	-0.229	0.214	-0.226	0.115	0.076	2.139		
VNIIM	3000	0.25	0.79	0.24	0.95	0.26	0.95	0.33	0.99	0.37	0.94	0.29	0.95		
VNIIM	7000	0.28	0.82	0.24	1.04	0.23	1.00	0.30	1.12	0.45	0.98	0.44	0.99		
VNIIM	10000	0.31	0.85	0.34	1.12	0.18	1.05	0.31	1.23	0.50	1.01	0.52	1.03		

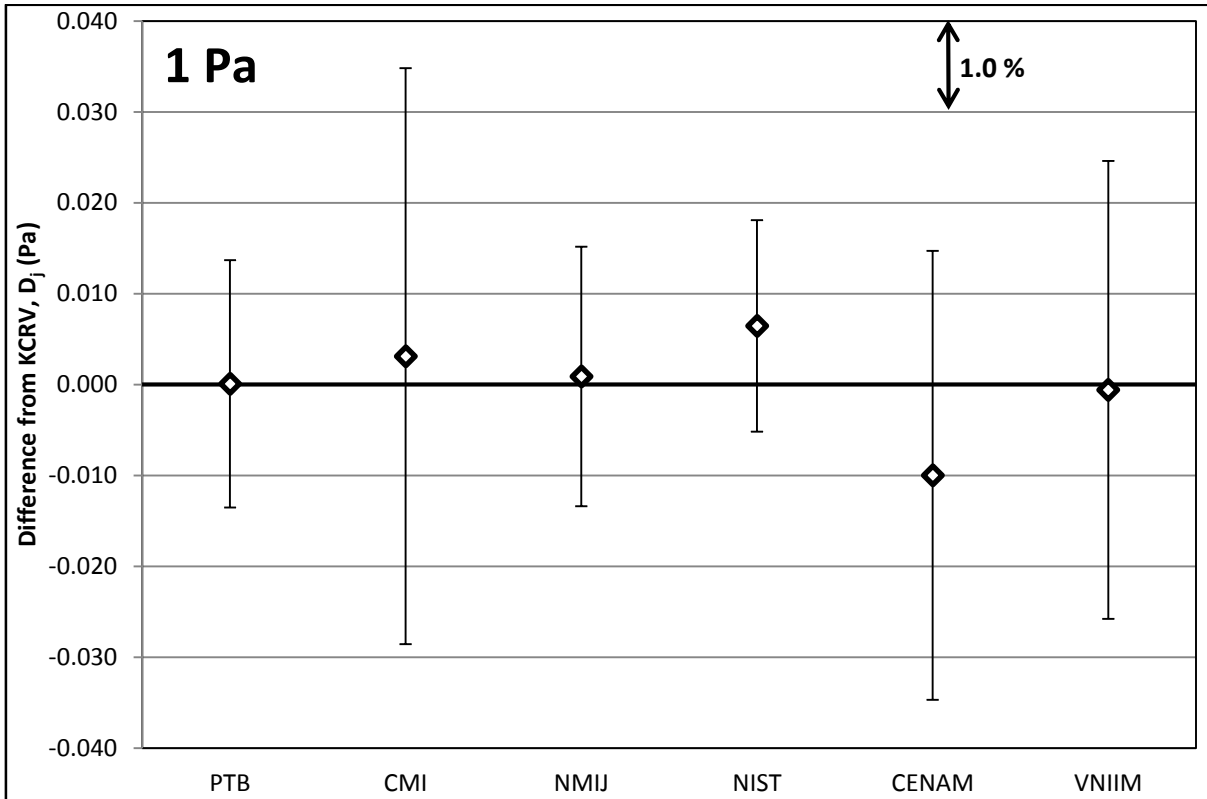


Figure 21. Deviations of corrected mean gauge readings from the key comparison reference values at 1 Pa. Uncertainty bars refer to combined expanded ($k = 2$) uncertainties of agreement between the NMI and KCRV.

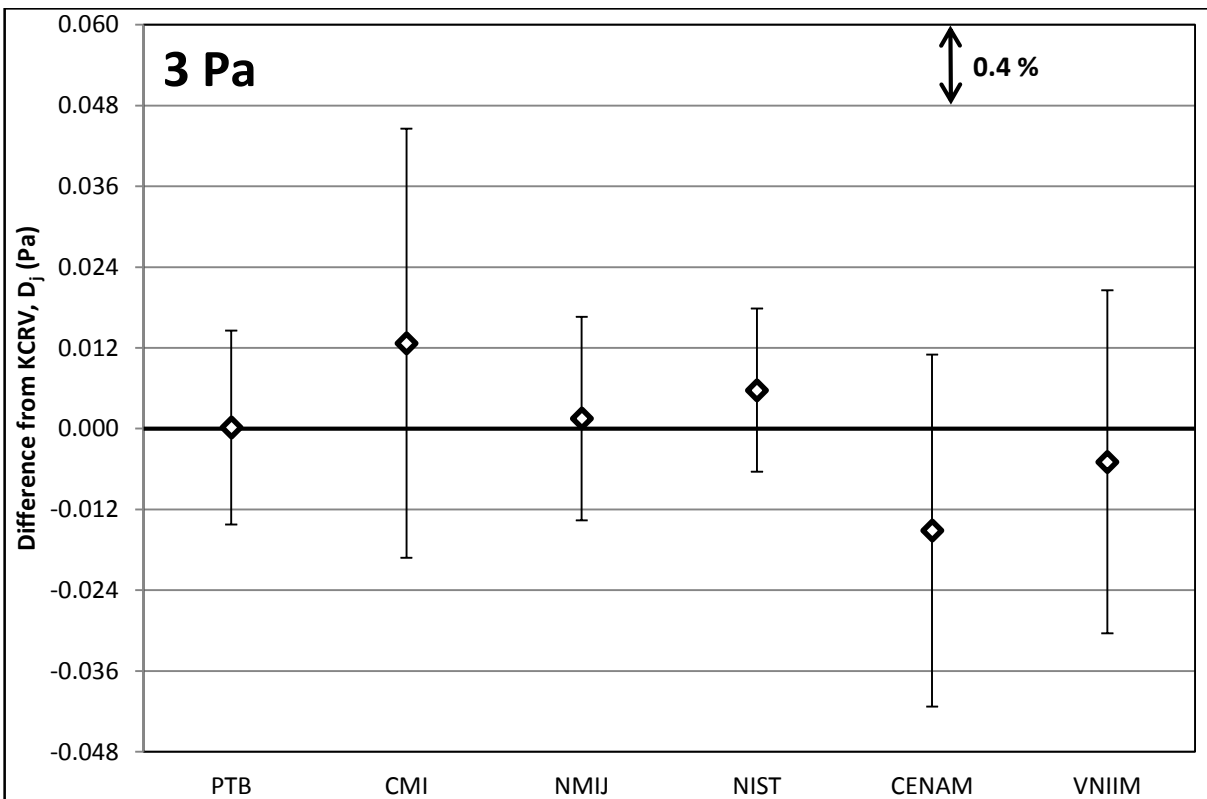


Figure 22. Deviations of corrected mean gauge readings from the key comparison reference values at 3 Pa. Uncertainty bars refer to combined expanded ($k = 2$) uncertainties of agreement between the NMI and KCRV.

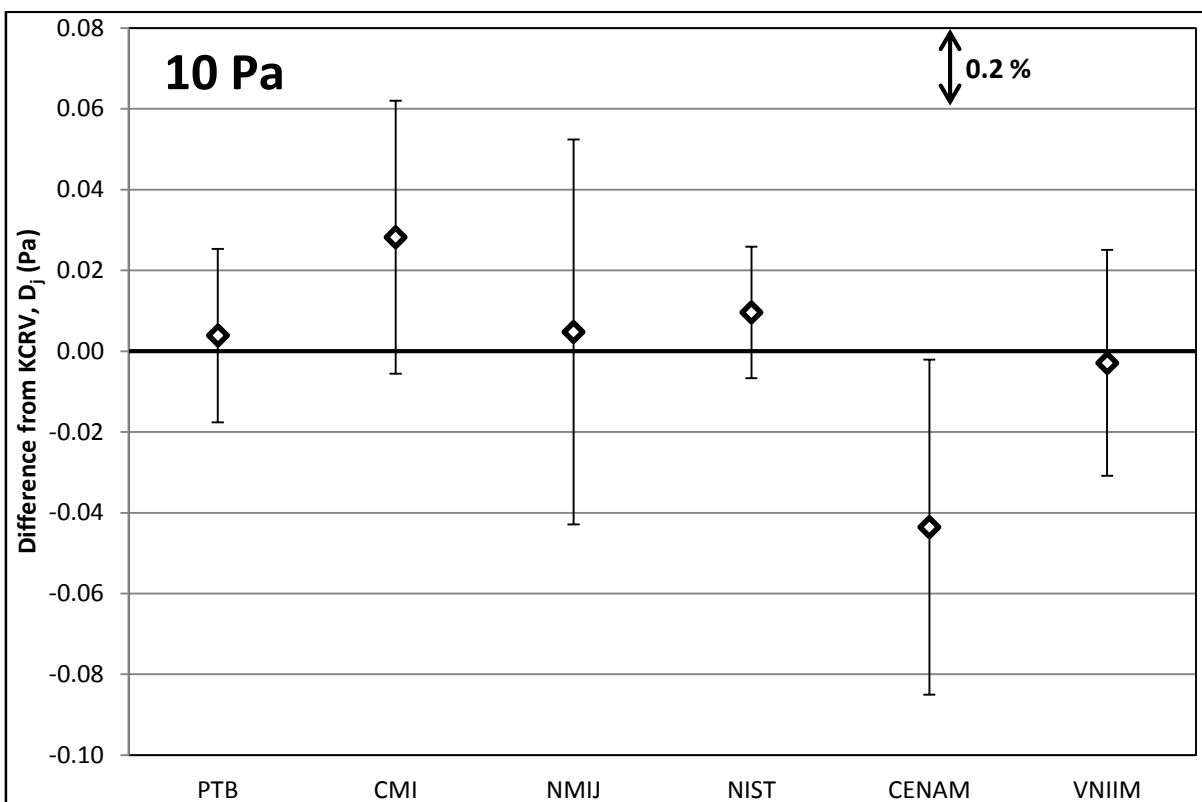


Figure 23. Deviations of corrected mean gauge readings from the key comparison reference values at 10 Pa. Uncertainty bars refer to combined expanded ($k = 2$) uncertainties of agreement between the NMI and KCRV.

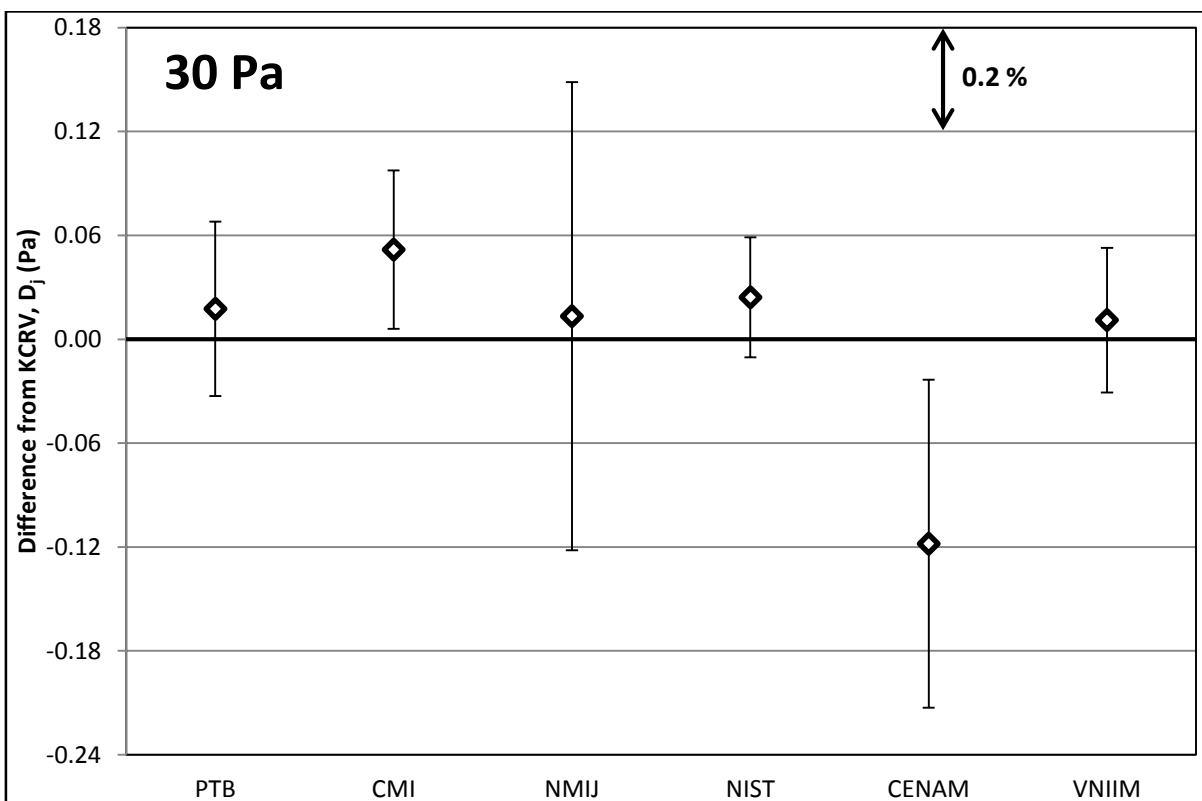


Figure 24. Deviations of corrected mean gauge readings from the key comparison reference values at 30 Pa. Uncertainty bars refer to combined expanded ($k = 2$) uncertainties of agreement between the NMI and KCRV.

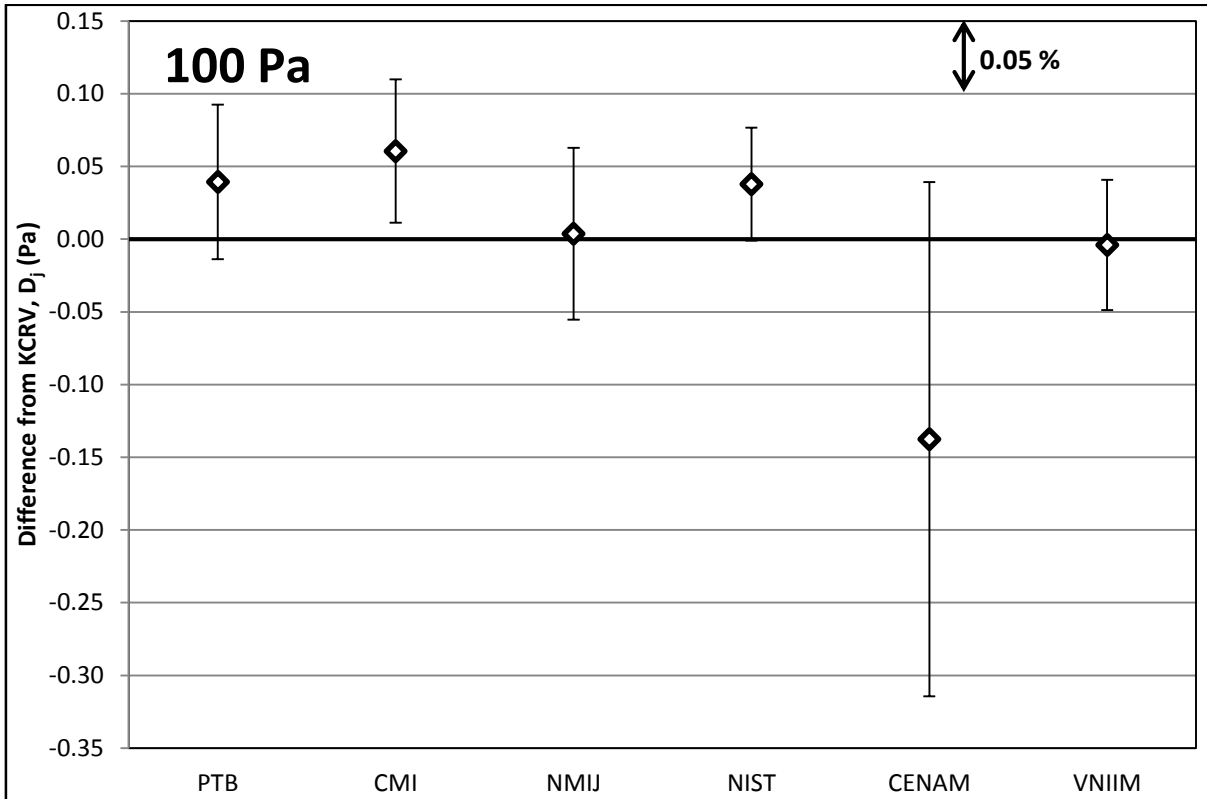


Figure 25. Deviations of corrected mean gauge readings from the key comparison reference values at 100 Pa. Uncertainty bars refer to combined expanded ($k = 2$) uncertainties of agreement between the NMI and KCRV.

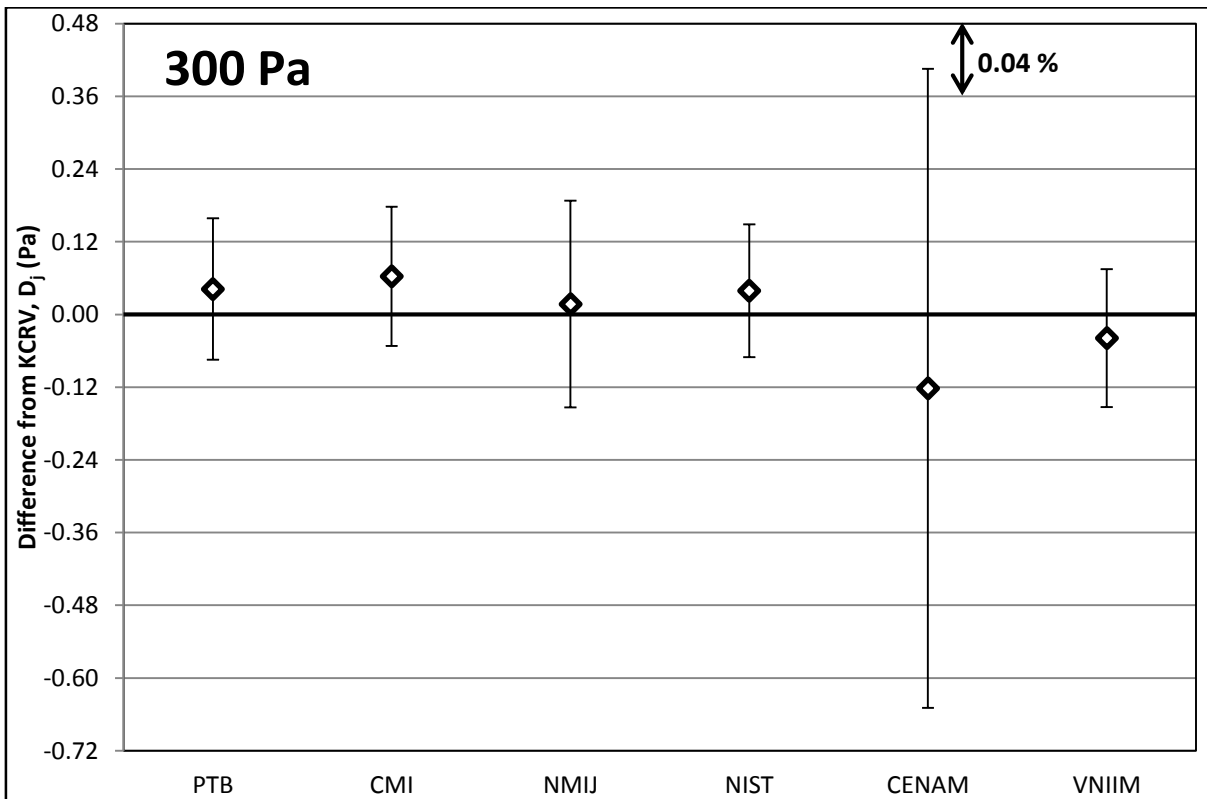


Figure 26. Deviations of corrected mean gauge readings from the key comparison reference values at 300 Pa. Uncertainty bars refer to combined expanded ($k = 2$) uncertainties of agreement between the NMI and KCRV.

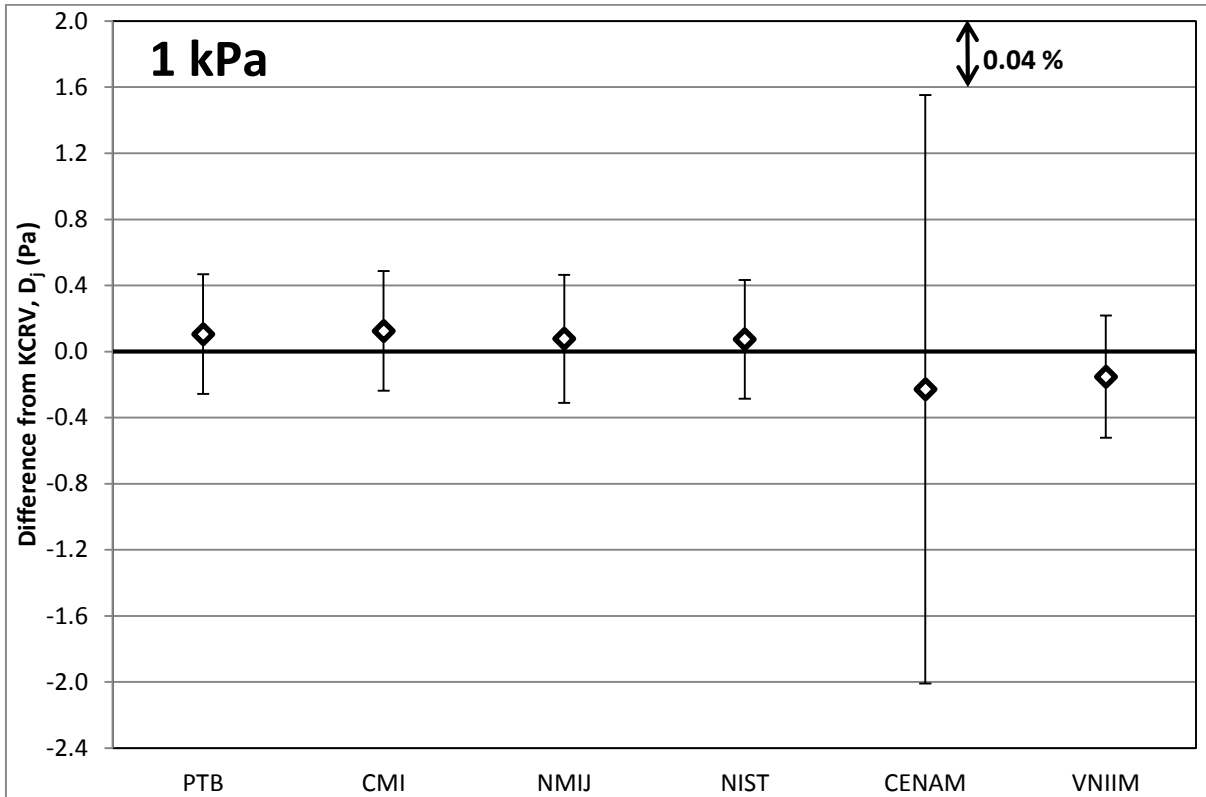


Figure 27. Deviations of corrected mean gauge readings from the key comparison reference values at 1000 Pa. Uncertainty bars refer to combined expanded ($k = 2$) uncertainties of agreement between the NMI and KCRV.

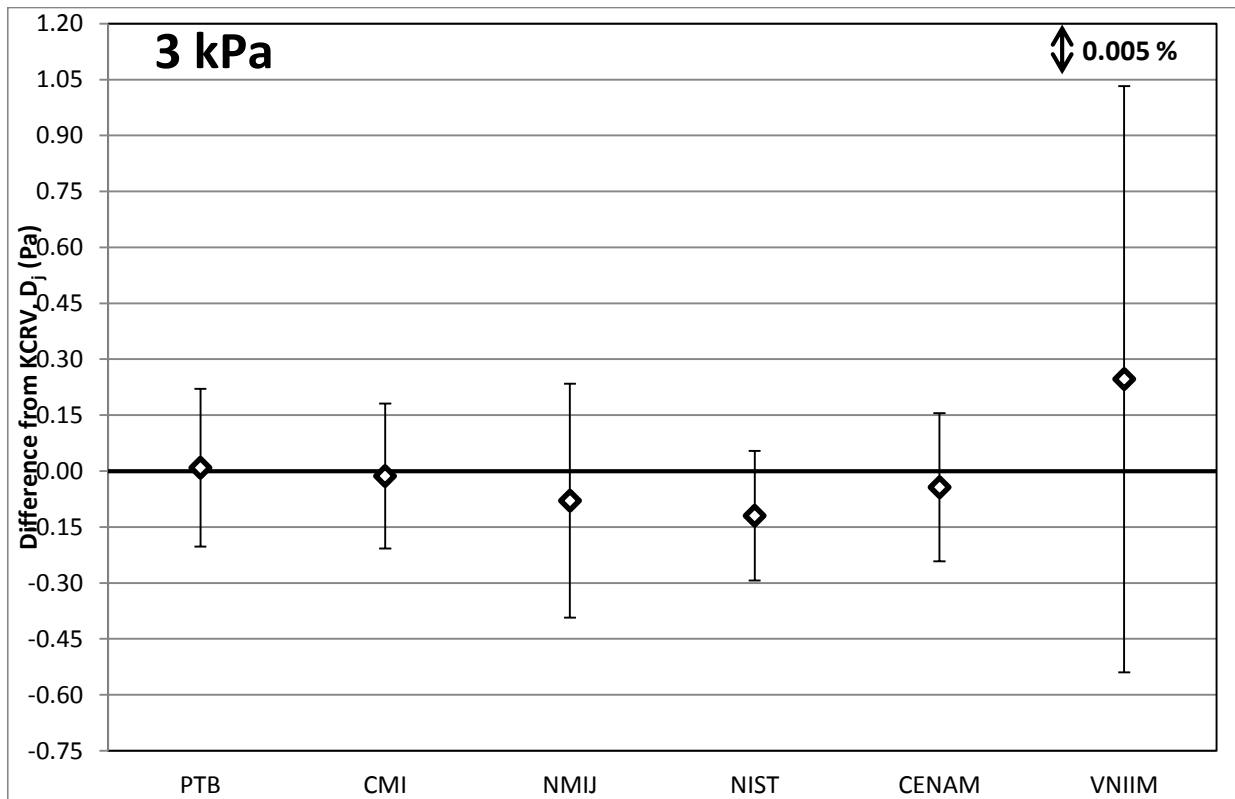


Figure 22. Deviations of corrected mean gauge readings from the key comparison reference values at 3000 Pa. Uncertainty bars refer to combined expanded ($k = 2$) uncertainties of agreement between the NMI and KCRV.

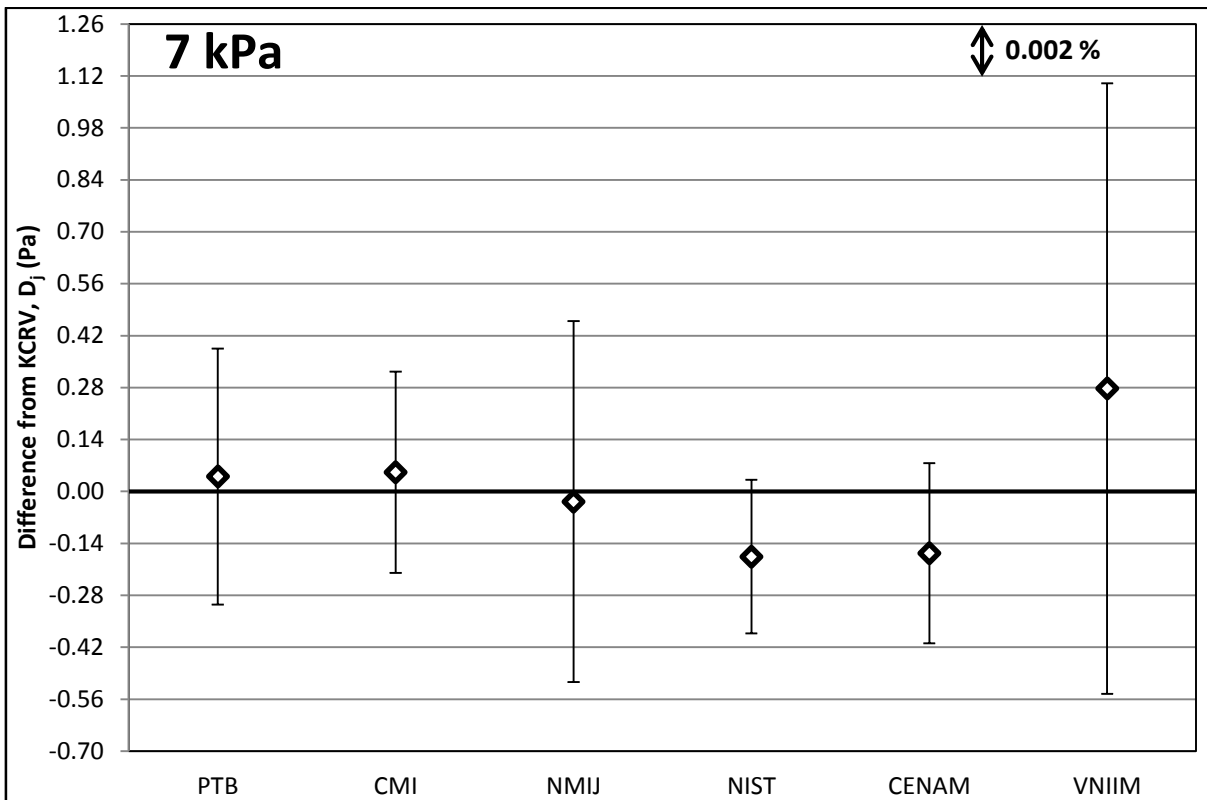


Figure 29. Deviations of corrected mean gauge readings from the key comparison reference values at 7000 Pa. Uncertainty bars refer to combined expanded ($k = 2$) uncertainties of agreement between the NMI and KCRV.

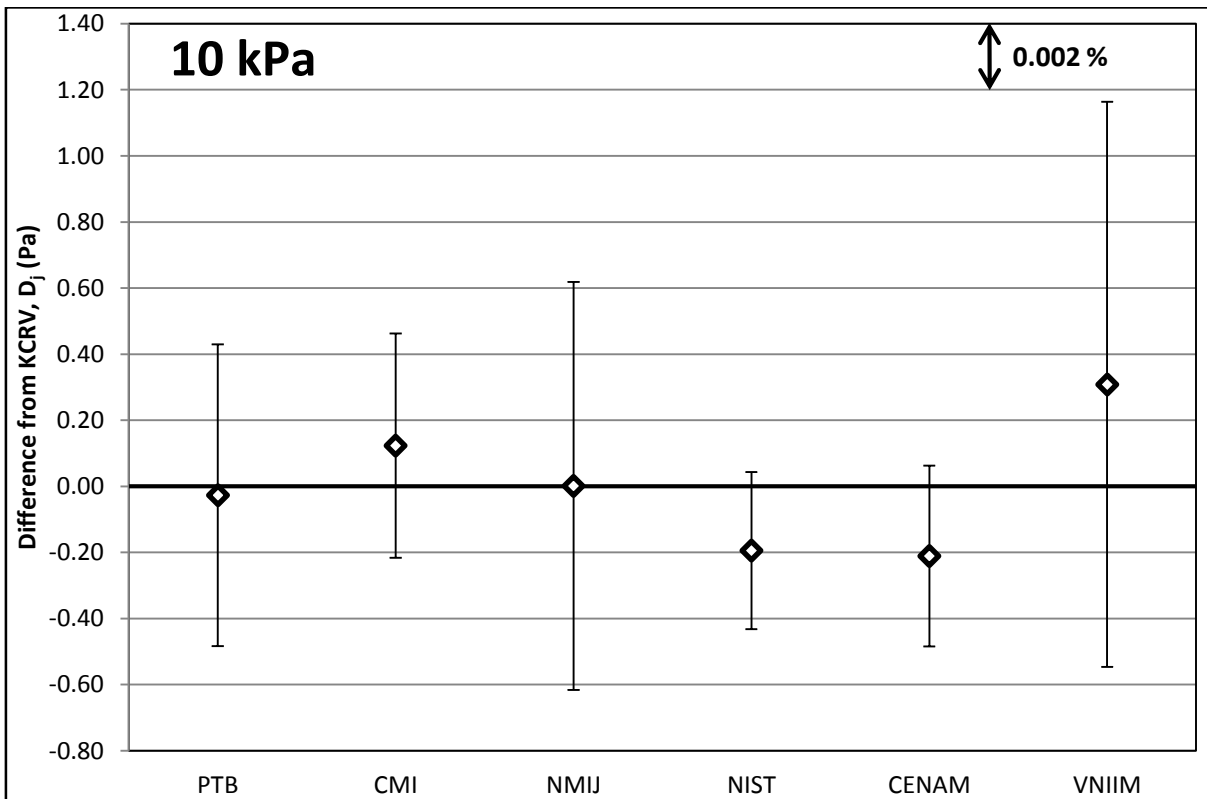


Figure 30. Deviations of corrected mean gauge readings from the key comparison reference values at 10000 Pa. Uncertainty bars refer to combined expanded ($k = 2$) uncertainties of agreement between the NMI and KCRV.

8. CONCLUSIONS AND DISCUSSION

Overall the comparison was a success, with the transfer package performing well and providing a stable artifact to compare laboratory standards. Of the comparisons outside the stated uncertainty, several of them have a marginal nonequivalence. However there are several cases where nonequivalence appears to be significant. The results considered significant have D_{jj} which are nonequivalent with a $k=3$ coverage factor. The pair wise comparisons which fall into this category are VNIIM vs PTB at 1000 Pa, VNIIM vs CMI at 300 Pa, VNIIM vs CMI at 1000 Pa, VNIIM vs NIST at 300 Pa, and VNIIM vs NIST at 1000 Pa.

For determination of the KCRV, several statistical methods were evaluated however methods such as weighted mean, which relies on the ability of every lab to accurately ascertain their uncertainty, and the laboratory effects model, which resulted in an open form solution (due to low number of participating labs and non-Gaussian distribution), didn't fit with this comparison. The statistical method chosen for the KCRV was the un-weighted mean, which is a very basic average of all labs; however it allows all laboratories an equal weight and chance to have agreement with the KCRV.

Pairwise comparisons indicate that VNIIM might have a problem at 300 Pa and 1000 Pa, however they have full agreement with the KCRV at those pressures. It should also be noted that VNIIM is operating a brand new standard and uncertainty estimation. Additionally, this is the top end of the VNIIM oil manometer, which is sometimes difficult to determine the uncertainty of density changes due to gas absorption in the oil.

Overall 93% of the data points taken had agreement with the KCRV and none were in disagreement at a $k=3$ coverage factor. Since there were only six labs determining the KCRV, the coverage factor is around 90% for $k=2$ and additionally since there is 100% agreement at $k=3$, we can assume that all labs with disagreements can be considered statistically equivalent with the KCRV.

ACKNOWLEDGEMENTS

Contributions by the following people should be acknowledged, in particular, T. Gooding (NIST), for assisting in reconstruction of the transfer standard, G. Strouse (NIST), for the assistance with the carnet, D. Olson (NIST), and K. Kousten (PTB), for review and KCRV discussions along with B. Toman (NIST) and W. Guthrie (NIST) of the Statistical Engineering Division at NIST, for advice on statistical methods. Several essential contributions were made at participating labs and we wish to thank A.I. Eichwald (Saint Petersburg State University) for help at VNIIM, Kenta Arai (NMIJ) and Momoko Kojima (NMIJ) for contributions at NMIJ, and finally Krajiček Zdeněk (CMI) and Martin Vičar (CMI) for involvement at CMI.

REFERENCES

1. Miiller A.P., Bergoglio M., Bignell N., Fen K.M.K., Hong S. S., Jousten K., Mohan P., Redgrave F. J., and Sardi M., "Draft B Report on the Key Comparison CCM.P-K4 in Absolute Pressure from 1 Pa to 1000 Pa", November 20, 2001.
2. Hendricks J.H., Olson D.A., "1 Pa– 15,000 Pa Absolute mode comparisons between the NIST ultrasonic interferometer manometers and non-rotating force-balanced piston gauges", *Measurement*, 43 (2010) 664-674.
3. Hendricks J.H., Miiller A.P., "Development of a new high-stability transfer standard based on resonant silicon gauges for the range 100 Pa to 130 kPa", *Metrologia* 44 (2007) 171-176.
4. Hendricks J.H., Olson D.A. "Towards Portable Vacuum Standards", *Physics World, Vacuum Challenges and Solutions*, 18-19, August, 2009.
5. Hendricks J.H., Ricker J.R., Chow J.H., Olson D.A., "Effect of Dissolved Nitrogen gas on the Density of Di-2-Ethylhexyl Sebacate: Working Fluid of the NIST Oil Ultrasonic Interferometer Manometer Pressure Standard" *Measure*, Vol.4 No.2, June 2009 52-59.
6. Tilford C. R., Miiller A. P., Lu S., "A new low-range absolute pressure standard", *Proc. 1998 NCSL Workshop and Symposium, National Conference of Standards Laboratories, Boulder, CO, USA*, 245-256.
7. Miiller A.P., Tilford C.R., Hendricks J.H. "A Low Differential-Pressure Primary Standard for the Range 1 Pa to 13 kPa", *Metrologia* 42 (2005) S187-S192.
8. Tilford C.R., "The speed of sound in a mercury ultrasonic interferometer manometer", *Metrologia*, 1987, 24, 121.
9. Jitschin W., Migwi J.K., Grosse G., "Pressures in the high and medium vacuum range generated by a series expansion standard", *Vacuum*, 1990, 40, 293-304.
10. Jitschin W., Migwi J.K., Grosse G., *Vacuum*, "Gauge calibration in the high and medium vacuum range by a series expansion standard", 1990, 41, 1799.
11. Jousten K., Rupschus G., *Vacuum*, "The uncertainties of calibration pressures at PTB", 1993, 44, 569-572.
12. Bock Th, Ahrendt H, Jousten K., "Reduction of the uncertainty of the PTB vacuum pressure scale by a new large area non-rotating piston gauge", *Metrologia* 46 (2009), 389...396.
13. Zdeněk Krajiček, Mercede Bergoglio, Karl Jousten, Pierre Otal, Wladimir Sabuga, Sari Saxholm, Dominik Pražák, Martin Vičar, "Final report on EURAMET.M.P-K4.2010 – Key and Supplementary Comparison of National Pressure Standards in the Range 1 Pa to 15 kPa of Absolute and Gauge Pressure", *Metrologia* 51 (2014), 07002 doi:10.1088/0026-1394/51/1A/07002
14. Delajoud, P., Girard, M.: *Vakuum in Forschung und Praxis* 15 (2003), 24-29.

- 15 Tesar, J., Repa, P., Prazak, D., Krajicek, Z., Peksa, L.: Vacuum.76 (2004), 491-499.
- 16 Torres-Guzman, J.C., Santander, L. A., Jousten, K.: Realisation of the medium and high vacuum primary standard in CENAM, Mexico, Metrologia 42(6) (2005), S157-S160
- 17 Sadkovskaya I.V., Eichwald A.I. “A laser interferometric oil manometer as the primary standard for absolute pressure in the range 1-1000 Pa”, Journal of Physics: Conference Series (JPCS) 2008, V.100, 092006.
- 18 Sadkovskaya I.V., Eichwald A.I. “The construction of floats for laser interferometric mercury manometer – new primary standard of Russian Federation in the range 0,1 – 130 kPa”, Abstract book of 19-th International Vacuum Congress (September 9-13, 2013, Paris, France), Posters. VST-P1-14.
- 19 Müller A P., “Measurement performance of high-accuracy low-pressure transducers”, Metrologia, 1999, 36 (6), 617-621.
- 20 Poulter K.F., Rodgers M.-J., Nash P.J., Thompson T.J., Perkin M.P., “Thermal transpiration correction in capacitance manometers”, Vacuum, 1983, 33 (6), 311-316.
- 21 Takaishi T., Sensui Y., “Thermal transpiration effect of hydrogen, rare gases and methane”, Trans. Faraday Soc., 1963, 59, 2503-2514.
- 22 Comité International des Poids et Mesures (CIPM), Mutual recognition of national measurement standards and of calibration and measurement certificates issued by national metrology institutes, 1999, Paris, pp.45.
- 23 ISO, Guide to the Expression of Uncertainty in Measurement (International Organization for Standardization, Geneva, Switzerland, 1993).
- 24 Taylor B.N., Kuyatt C.E., Guidelines for Evaluating and Expressing the Uncertainty of NIST Measurement Results, NIST Technical Note 1297, 1994 Edition (U.S. Government Printing Office, Washington, 1994).
- 25 Youden W.J., “Graphical diagnosis of interlaboratory test results”, Industrial Quality Control, 1959, 15 (11), 24-28.